University of Padova

Department of Astrophysics and Cosmology

Master Thesis in Irradiation Environment for Planets in Habitable Zone

Supervisor
Prof. Giampaolo Piotto
University of Padova

Co-supervisor
Prof. Riccardo Claudi
University of Padova

Master Candidate
Golnar Mirzad

Student ID
2005896

Academic Year
2023-2024

Contents

Abstract

This thesis explores the complexities of cosmic habitability, investigates the influence of M-dwarf stars, the role of high-energy radiation and water, as well as the likelihood of water loss during different planetary phases. Specific attention is given to the habitability of Proxima b and TRAPPIST-1's planets and the factors governing their habitable zones.

Chapter 5 presents original research. Initially, primary conditions are considered to identify target exoplanets. Subsequently, detailed evolutionary models are created. Factors such as luminosity, age, and the inner distance of planets are then analyzed, considering two different models and four different amounts of fluxes that planets could receive in various phases of their lives. Following this, the investigation shifts to determining the duration that planets spend outside the habitable zone before transitioning into it and makes approximate about the amount of water mass planets have lost in those duration comparing to TRAPPIST-1 and Proxima b. This provides valuable insights into the temporal aspects of habitability.

These investigations offer a nuanced understanding of the interplay between stellar characteristics, planetary conditions, and the temporal dynamics of habitable zones. This thesis contributes to existing knowledge and sets the stage for future exploration in the captivating field of cosmic habitability.

Chapter 1

Introduction

Searching for life beyond Earth is considered a highly important and meaningful undertaking within the field of science for many years. This increasing interest has driven the development of the next generation of astronomical facilities and instruments aimed at detecting biosignatures indicating the presence of life and technosignatures that could offer evidence of intelligent life. Our discoveries within our solar system, such as the presence of liquid water on Europa and Enceladus, frozen water in the polar caps of Mars, and the detection of organic compounds in comets, asteroids, and meteorites, all increase the likelihood of the existence of life beyond Earth. Beyond our solar system, the prospects of finding extraterrestrial life seems even more promising, with the growing number of exoplanets(5,539 until November 2023)and counting discovered within the Milky Way.

Over the years, numerous exoplanets have been discovered through various detection methods that some of these planets are situated in the habitable zone (HZ), a region around a star where a terrestrial-mass planet with a CO_2–H_2O–N_2 atmosphere could maintain liquid water on its surface (Kopparapu et al., 2013). The HZ model, based on the star's temperature and the amount of radiation reaching the planet, has been instrumental in determining the extent of planets with Earth-like conditions and their potential to support extraterrestrial life(Soliz, 2023).

Presence of liquid water is a primary requirement which is dependent on surface temperature(Squicciarini et al., 2021). Therefore, orbital distance and luminosity of its parent star are the crucial parameters to control the temperature of a planet, but there are other crucial factors necessary for a planet to be habitable and possess Earth-like qualities. These include a dense atmosphere capable of sustaining liquid water. Venus and Mars can't have liquid water on their surfaces. Venus is too hot because its thick atmosphere traps heat, while Mars is too cold since its thin atmosphere can't keep enough heat, causing water to freeze or evaporate quickly(Gordon and Sharov, 2017). the presence of suitable greenhouse gases to maintain the right temperatures, an active magnetic field, and the existence of organic compounds are the other factors. Investigating the presence and levels of oxygen is an important factor in determining habitability, especially for supporting complex life forms such as plants and animals. In fact, one of the most significant bioenergetic innovations in the history of life on Earth was the development of oxygenic photosynthesis by cyanobacteria.

Exoplanets, planets outside our solar system, likely need similar things to support life for a long time. Scientists studying life on Earth found three important things that all living things need: (1) a source of energy, like sunlight or chemicals; (2) specific elements like carbon, hydrogen, nitrogen, oxygen, phosphorus, and sulfur that make up living things; and (3) water for chemical reactions. Knowing these basics, we can think about what makes a place habitable. This brings up questions about how Earth stays habitable, how planets form, and what conditions in space

help or limit the possibility of life (Gordon and Sharov, 2017).

The discovery of exoplanets and their arrangements has been facilitated through methods such as radial velocity and planetary transit (Saar et al., 1998; Charbonneau et al., 1999). These observations are outcomes of the planet formation process that takes place within protoplanetary disks (Pollack et al., 1996; Boss, 1997; Matsuo et al., 2007). Models striving to elucidate the development of planets from protoplanetary disks seek to align fundamental physical processes with planetary configurations resembling the Solar System and other explanatory systems. Alongside observations, these models suggest a wide spectrum of potential planetary arrangements that differ significantly from our Solar System.

When we look beyond Earth's requirements for life and explore environments that can support life, we discover that life itself plays a big role in shaping its surroundings. For example, early life on Earth survived without oxygen, but as plants produced more oxygen through photosynthesis, new types of life adapted to using oxygen. Using oxygen helps life become more efficient.

This tells us that biology (life science) is closely connected to how things work in the physical world, and life's ability to change its surroundings isn't random but has reasons behind it.

Now, if we know that habitable (livable) conditions are important for life, and life is crucial for keeping those conditions good over a long time, we wonder: How can we study what makes a place habitable without first understanding how life began?

When we talk about making places suitable for life, we want to make sure they stay that way for a long time. It's important to be specific about the kind of life we're interested in and the environment it needs. For example, Europa, one of Jupiter's moons, is interesting because it might have liquid water beneath its frozen surface. The heat there comes from the way Europa moves around Jupiter.

As we explore what makes places habitable, we need to consider the limits, how life changes its surroundings, and the uncertainties when we apply what we know about life on Earth to other places in our Solar System or Galaxy. Now, let's look into how our Galaxy, the Milky Way, supports habitability.

While we understand what life needs on Earth by studying different environments, figuring out if other places can support life is more challenging. For instance, when scientists look for planets outside our solar system, they might say they found a habitable planet just because it's in the right zone, even without knowing other important details like its atmosphere. Sadly, until we have better tools in the future to measure things like signs of life or other factors, we can only get a general idea of how habitable our Milky Way really is.

Defining the zone of enhanced galactic habitability proves to be a more intricate task than establishing the habitable zone of a Main Sequence star. The central goal is to pinpoint specific regions within the Galaxy capable of sustaining habitable conditions for extended durations.

The galactic habitable zone (GHZ) concept was initially introduced by Gonzalez et al. (2001), marking the commencement of extensive exploration over the past decade. The GHZ parallels the habitable zone (HZ) concept but is tailored to the Milky Way. Originally, it was conceptualized as an annular region with the potential to host habitable planets strategically positioned away from the Galaxy's center or periphery. The inner edge is believed to be restricted by frequent transient radiation events, while the outer edge faces limitations due to insufficient metallicity crucial for planet formation. Consequently, a habitable planet is one capable of maintaining an environment free from transient radiation events for timescales pertinent to surface-dwelling life. However, the impact of such events on subsurface or aquatic life remains uncertain.

When considering the habitability of a planet within the Milky Way, the focus is on conditions that may support complex life on land. The term "galactic habitable zone" designates regions

in the Galaxy with the highest capacity for sustaining complex life over time. Delving into the influence of astrophysical events on the habitability of planets contributes a small part to our broader understanding of the Milky Way's habitability over cosmic time and our species' precarious position on Earth.

We're still figuring out if the Milky Way could be a good home for life. To explore this on a big scale, we look at habitability as a place's ability to handle sudden radiation events that can harm a planet's atmosphere. Many stars have planets similar in size to Earth, and it's interesting that these planets can form without needing a lot of metals. This means Earth-like planets are scattered across the entire Galactic disk and come in different ages. In the vast Milky Way, there's a chance many planets haven't been affected by big events like supernovae (SNe) and long gamma-ray bursts (GRBs). Predictions in this area are still changing, and future observations checking what's in planetary atmospheres and looking for signs of life could help us find planets that are truly habitable.Exploring the history of our solar neighborhood through galactic archaeology studies can tell us how often planets survive big astrophysical events. When we think about how the galaxy moves, we realize habitable planets might be in different galactic environments as time goes on.These new discoveries will make our understanding of big-scale habitability more complicated, but they'll also help us figure out if there's a chance for life in our Galaxy and the wider Universe.

In this regard, we firstly, delve into the intricate details of M-dwarf stars in chapter 2, exploring their characteristics and the sources of high-energy radiation they emit. Understanding the nature of these stars is fundamental to comprehending their influence on the habitability of surrounding exoplanets.

Then we will shift the focus to the pivotal role of water in determining habitability. We examine the various aspects of water, ranging from its presence on exoplanets to its potential impact on creating and sustaining habitable conditions.

Then in Chapter 4, we will talk about the detailed investigation of specific planetary systems, particularly Proxima Centauri and the TRAPPIST-1 planets. By scrutinizing these systems, we aim to uncover insights into their potential habitability and the factors influencing their habitable zones.

In Chapter 5, we begin from identifying target exoplanets, plotting luminosity-age diagrams, and analyzing the evolution of inner distances. Additionally, we explore the crucial concept of timing, examining the duration planets spend within the habitable zone before entering it and approximate the water mass loss that plants might have experience before entering HZ.

at last we will talk about the result we took, in section of Summary. Through these chapters, we aim to provide a comprehensive understanding of the complex interaction between stellar characteristics, planetary conditions, and the quest for habitable exoplanets. Each chapter contributes a unique perspective to our overarching goal of unraveling the mysteries of explanatory habitability.

Chapter 2

M stars and Sources of High Energy Radiation

In this chapter we will explore the fascinating world of M-dwarf stars and the energetic radiation they emit. We look into the different sizes and brightness levels of these stars, trying to understand the complex changes they undergo over time. By doing so, we discover the interesting elements that influence their surroundings. This chapter enhances our overall understanding of the various types of energetic radiation, giving us a better view of the cosmic stories that develop as we continue our exploration.

2.1 M-stars

M-type stars, commonly denoted as red dwarfs, hold the spotlight as the most abundant stellar entities in the cosmos, representing the smallest cadre of stars that engage in hydrogen burning. Their masses fluctuate in the range of roughly 0.08 to 0.6 times that of the Sun. Within the tapestry of the Milky Way Galaxy, red dwarfs command a substantial presence, comprising about three-fourths of the stellar population, and this preeminence escalates even further in elliptical galaxies. These modest stars showcase a radius that falls within the spectrum of 0.3 to 0.7 times that of the Sun. Their luminosity spans a modest range, clocking in at 0.01 to 0.08 times the Sun's luminosity, while their surface temperatures exhibit a variance from 2,400 K to 3,790 K. Adding to their allure, red dwarfs boast an extraordinary lifespan, enduring from 1 to 10 trillion years. M stars exhibit distinctive spectral features, primarily dominated by prominent lines originating from diatomic molecules like TiO, VO, and MgH. In contrast, the absorption lines associated with hydrogen in these stars are either extremely faint or entirely absent. Strong lines from sodium and neutral metals such as CaI and FeI are also observed in the M-stars spectra.

For a planet orbiting an M-star to harbor liquid water on its surface, it needs to maintain close proximity to its parent star. However, the prevalent challenge stems from the intense and frequent flaring activity characteristic of these stars, leading to the assumption that such planets are likely tidally locked, resulting in atmospheric freeze-out on their dark side(Scalo et al., 2007) Consequently, M-stars were long deemed improbable candidates for habitable planets. Joshi et al. (1997) suggested that the transportation of heat within the atmosphere could counteract freezing on the dark side. Their models demonstrated that atmospheric circulation between the light and dark sides could sustain atmospheres with thicknesses as minimal as 0.1 bar, while thicker atmospheres, ranging from 1 to 2 bar, could support the presence of liquid water across a substantial portion of

the surface. Notably, their 2003 models even entertained the possibility of water worlds entirely shrouded in oceans, accompanied by tolerable wind speeds ranging between 10 and 20 m/s. It is crucial to recognize the overlooked aspect of tidal forces around M stars. Beyond the conventional understanding that these forces might lead to planetary tidally locking, they also play a role in circularizing planetary orbits within the habitable zone. Additionally, they could contribute to dampening chaotic obliquity fluctuations, akin to how the Moon stabilizes Earth's axial variations. This nuanced consideration adds depth to our comprehension of the dynamic interplay shaping planetary conditions around M-type stars.

According to look into different aspects of living around M stars, Heath et al. (1999) explored the possibility of creating atmospheric ozone without life to protect against star flares.Significantly, they stressed he shift of starlight to the red spectrum doesn't necessarily block or hinder the process of photosynthesis. Finding many planets outside our solar system and seeing how well certain tiny living things can adapt got scientists excited again about M stars. They're the most common stars near us and probably in our whole galaxy. So, scientists started looking again to see if there might be life-friendly planets around them. Furthermore, scientists got even more excited when they found significant occurrence of (possibly) protoplanetary disks around very young M stars. They also discovered strong signs that planets might be around M stars and identified a bunch of Neptune-like planets and two big planets orbiting M stars—5 to 7 times the mass of Earth.

2.1.1 M stars' broad spectrum of masses

Regarding astronomy classifications, the category of M stars does not have a clear and unified definition. And it is primarily based on the prevalence of molecules in the spectra of their photospheric spectra. The most fundamental attribute that governs the majority of M stars' characteristics and progression throughout its lifespan is their mass. As it is mentioned in the previous section, M stars cover a spectrum of masses, ranging from 0.6 to 0.08 sun mass. In fact, the upper boundary of them is arbitrary but their lower limit is considered to be the boundary that defines brown dwarfs. Indeed, Objects with lower masses undergo degeneracy before they can initiate hydrogen fusion, As a result, they gradually fade and cool over time without experiencing the slowdown in evolution observed in nuclear-burning stars. That is the why their luminosities compare to the faintest main sequence M stars are quite rare and until recently, observation of them even with the largest telescope was challenging. In contrast, the M9 stars, which are the least massive among M stars, are capable of hydrogen burning and can sustain a relatively constant luminosity for a staggering duration of at least 100 billion years.Therefore, it is evident that a natural distinction exists between M9 main sequence stars and brown dwarfs, highlighting a clear boundary between the two categories. The fundamental property that underlies the basic characteristics of M stars, as well as many considerations related to habitability and planet exploration, is the wide range in mass, which spans a factor of 7. This mass range forms the foundation from which various properties and investigations concerning M stars and their potential for habitable environments and planetary discoveries stem. The ratio of mass intervals within the M star category is larger compared to the combined spectral types AFGK. This significant mass interval ratio contributes to the fact that M stars are, without a doubt, the most abundant stars per unit volume in the Galaxy. This assumption holds true under the condition that the initial mass function remains consistent across different positions within the galaxy. It is worth noting that comprehensive counts of M stars are available only for stars within a distance of approximately 5-10 parsecs.

2.1.2 M stars' luminosity and effective temperature

One of the most significant characteristics of M stars is their wide range of luminosity that is as a result of extensive variation of them in mass. Fig. 3.2 shows the correlation between mass and luminosity, which is derived from a compilation of binary star masses along with selected luminosities(Scalo et al., 2007).

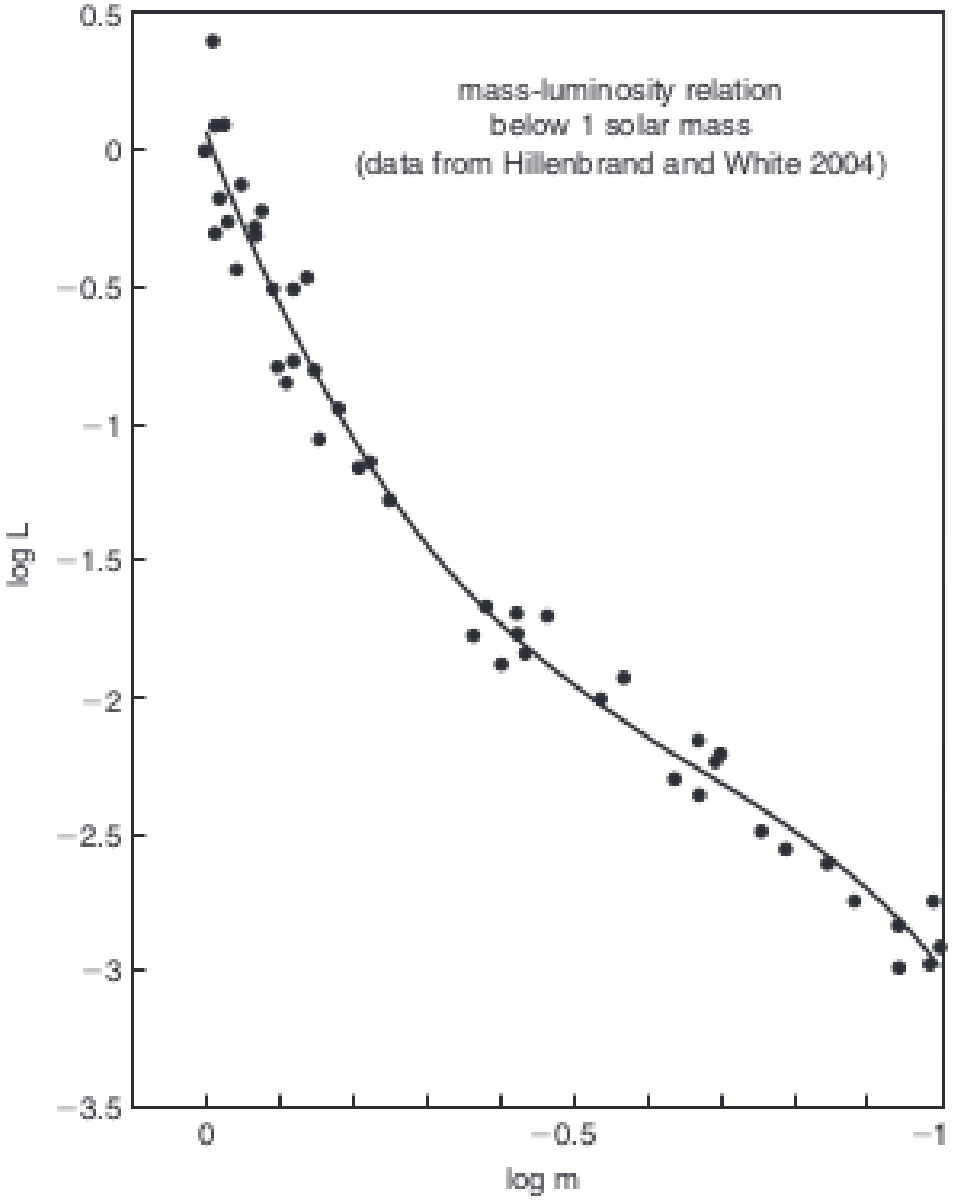

Figure 2.1: Mass-luminosity relation for main sequence stars which have similar mass as sun(Scalo et al., 2007)

A practical polynomial fit to the data,is given by

$$logL = 4.10(logM)^3 + 8.16(logM)^2 + 7.11logM + 0.065(1)$$

L and M are in solar units. L $\simeq$ M^3, is considered as a rough fit to the data within the range of

0.1 to 1 $M_\odot$ for illustrative purposes. T The broad range of bolometric luminosity in M stars, influenced by their mass, results in a factor of about 100 difference. Even the most luminous M star, categorized as spectral type M0, is over 10 times dimmer than the sun. Detecting M stars with the lowest luminosity proves challenging, especially in more distant areas. Consequently, the detection of planets around M stars becomes a formidable task. Another unique feature of M stars lies in their effective temperature (T_{eff}), varying from 3800K for M0 to 2500K for M9, with an approximate uncertainty of 100-200K(Scalo et al., 2007).

2.1.3 Possibility of Photosynthetic

While the total light emission remain relatively constant across M0 to M9 stars, there is a noticeable variation in the amount of visible light. This alteration in the visible spectrum could be significant when assessing its effects on living organisms. Planets with a substantial ozone layer face vulnerability to harmful radiation in the UVB range (280-315 nm). However, a notable portion of overall radiation damage takes place in the UVA spectrum (315-400 nm), extending even into the visible light range.

For planets around M-type stars with an ozone layer, the main concern is the visible and UVA range of radiation, not UVB like on Earth. This change happens because the intensity of radiation decreases sharply when move towards the blue and visible part of the spectrum. The elongated part of the action spectrum for biological effects, linked to oxidative damage, becomes more noticeable as the planet's surface spectrum pass through the point where ozone absorbs radiation.

However,The low effective temperatures of M stars will be cause the existence of liquid water in the planet located in a suitable distance, but the question is whether the luminosity that planet receives in the specific wavelength ranges is enough for photosynthesis. Main responsible for generating oxygen on Earth is photosynthesis which breaking down water molecules using light-catching mechanisms.This process plays a vital role in keeping the oxygen balance in our atmosphere, thanks to complex interactions with geological processes. Figuring out the exact amounts of oxygen on Earth and on planets around M stars is a significant challenge(Scalo et al., 2007).

A comprehensive study that delved into the growth, adaptation mechanisms, and photosynthetic efficiency of certain strains of cyanobacteria under simulated light conditions resembling those of M-dwarf stars has shown that both tested cyanobacteria can thrive and perform photosynthesis effectively under such simulated lighting. The calculations have indicated that exoplanets that are tidally locked within the habitable zone of M-dwarf stars would receive an adequate amount of visible light photons to support photosynthesis, similar to that on Earth. The productivity is estimated to range between 13% and 22% of the levels seen on Earth(Battistuzzi et al., 2023).

2.1.4 Variation in long time

The radiation a planet receives from its host star plays a crucial role in shaping its climate, atmospheric composition, and potential for sustaining life. Therefore, understanding variations in the star's behavior over time is essential in assessing a planet's habitability. While our Sun occasionally experiences intense flares and high-energy particle events, these short-term fluctuations have, for the most part, had limited impact on Earth, except for some disturbances in the upper atmosphere.

In contrast, the chemistry of the stratosphere can be affected at high latitudes, leading to variations in substance transport from polar regions, especially on planets with synchronous ro-

tation lacking a polar vortex to contain these changes. The Sun, having gradually increased in brightness since entering a hydrogen-burning state, poses a challenge known as the "faint young sun" paradox. Even with 30% less luminosity four billion years ago, Earth would have entered a challenging-to-reverse "snowball" phase due to this rise in solar brightness.

On the other hand, planets orbiting M stars don't face this dilemma. The luminosities of M stars remain remarkably stable over extremely long periods once they enter the main sequence, excluding the pre-main sequence phase. Evolutionary calculations by Laughlin et al. (1997) suggest main sequence lifetimes for low-mass stars ranging from 10^{11} to 10^{13} years. During the main sequence phase, most M stars undergo minimal brightening, and notably, they never enter the red giant phase. Consequently, the habitable zone with liquid water doesn't experience radial expansion for planets orbiting M stars.

2.1.5 Atmosphere

When a planet is in the right zone around an M star, there's a special situation because it always shows one side to the star. This means one side is always warmer (day side), and the other side is always colder (night side). Without something moving heat between these sides, the night side could get so cold that things in the air might turn into liquid and fall to the ground. But, there are air processes that help keep the temperature difference between day and night sides lower by moving heat around(Claudi et al., 2016).

Some smart models and studies (Joshi et al., 1997) have shown that a planet with a thick enough atmosphere, especially one with a lot of CO_2 (like Earth's atmosphere), can keep the night side from getting too cold. This helps the planet have liquid water on a big part of its surface. Some scientists even thought about planets that might be all covered by oceans.

How much CO_2 is in the air and how it changes because of things like big movements in the planet's plates and volcanoes are really important for deciding what the weather is like on these planets(Kasting and Catling, 2003).

2.2 The limitation imposed by radiation on the potential for life

Several factors play a role in determining the possibility of life on planets. A critical aspect to consider in evaluating the potential for life to emerge and thrive is astrophysical radiation, which can act as a barrier to the origin and evolution of life. Additionally, the radiation received by the planetary body and the plasma environment created by its parent star are crucial elements that impact the planet's evolution and atmospheric conditions. Therefore, radiation becomes a significant factor in shaping the conditions necessary for the emergence, development, and sustainability of life on planetary bodies.

2.2.1 Types of radiation

Life in the universe faces the challenge of various radiation forms, including electromagnetic radiation and energetic particles. Among the electromagnetic radiation, gamma rays, X-rays, and ultraviolet radiation pose a threat to essential biological molecules like DNA and proteins. Energetic particles, such as electrons, protons, neutrons, and muons, also contribute to potential damage. Diverse processes generate high-energy electromagnetic radiation, while plasma shocks

and interactions with magnetic fields propel charged particles to high energies. Nuclear reactions, either from radioactive decay or interactions with high-energy primary protons, produce neutrons and muons. Certain radioactive decay processes yield helium nuclei and energetic electrons. Terrestrial planets with robust magnetic fields, like Earth, contain high-energy electrons in their magnetospheres. Moons orbiting giant planets may undergo significant irradiation from the planet's magnetospheric electrons, with ice or rock shielding helping to reduce impacts beneath the surface(Gordon and Sharov, 2017).

2.2.2 Source of high-energy radiation

Stellar emission

Radiation from stars takes on various forms, spanning visible light, UV, X-ray, and gamma-ray light, with the type and amount contingent on a star's surface temperature and activity level. High-mass stars, though emitting considerable UV, have limited lifespans, reducing the likelihood of hosting habitable planets. The focus for habitability shifts toward stars like the Sun (G and K types) and lower-mass stars (M type). Consider the Sun, emitting enough UV light to impact planets lacking a UV shield, such as ozone. Lower-mass stars emit less UV but showcase increased activity, often experiencing energetic flares that release UV, X-ray, and potentially gamma-ray light. These flares result from magnetic processes affecting various atmospheric layers, heating the plasma, and propelling particles. Stellar flares from low-mass stars can outshine solar flares in X-ray and EUV flux. The sporadic emission pattern from low-mass stars may pose challenges for life adaptation compared to a more consistent background emission. Over a star's lifespan, radiation emission changes; younger stars are less luminous but more active, generating frequent and intense flare events. As stars age, luminosity gradually increases, and activity tends to decrease, especially for higher-mass stars, while low-mass M-dwarf stars maintain high activity levels(Gordon and Sharov, 2017).

Stellar explosion

Stellar explosions are classified into supernovae and gamma-ray bursts (GRBs), based on their light emission. Supernovae are further categorized into Type I and Type II events, depending on their light curve and spectral features. Type Ia supernovae likely originate from the explosion of a white dwarf accreting matter from a companion star, while Type II events result from the core collapse of high-mass stars. Supernovae emit visible, UV, and likely higher-energy light, with gamma-rays originating from radioactive decay of synthesized elements. Neutrinos are a significant product of supernovae but interact weakly. Supernovae also create ejecta blast waves forming remnants visible for some time and injecting material into the interstellar medium, potentially influencing cosmic rays. GRBs are characterized by bursts of gamma radiation, categorized as long or short based on duration and spectral characteristics. Long GRBs are likely from core-collapse supernovae with intense material jets, while short GRBs are likely from compact object mergers. Other short-term stellar events, like soft gamma repeaters and active galactic nuclei, also emit high-energy radiation, influencing cosmic ray flux, but are less significant for habitability compared to supernovae and GRBs(Gordon and Sharov, 2017).

2.2.3 Effects

The impact of radiation on habitability depends on two main factors. First is the total energy absorbed by a particular habitat, and second is the "hardness" of the radiation. Hardness, in this context, refers to the mix of higher- to lower-energy photons or particles originating from the source. Consequently, the effects of radiation on life are determined by the type of radiation (electromagnetic or particle-based), their respective energy levels, the amount of radiation, and the ability of living organisms to adapt. These factors are succinctly summarized in Fig. 2.2.

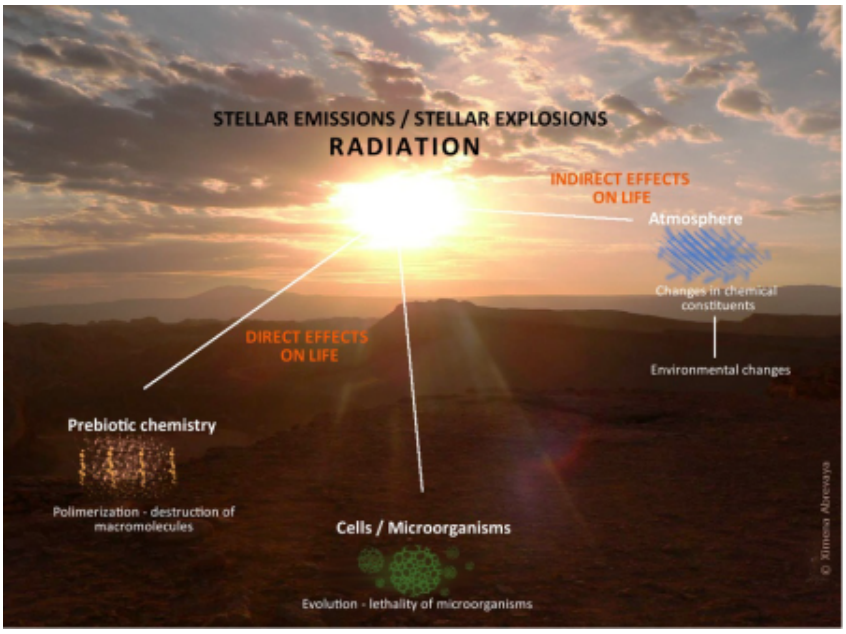

Figure 2.2: Sources of radiation and its impact on life through direct and indirect effects(Rampelotto et al., 2018)

The potential harm of radiation to a planet's surface biologically depends on the existence of a magnetic field and an atmosphere. The strength of a magnetic field and the characteristics of charged particles, such as their momentum and charge, determine its ability to shield against them.

The atmosphere's effectiveness in shielding against particle and electromagnetic radiation is influenced by the energy level of the radiation and the thickness of the atmosphere(Dartnell, 2011).

Impacts on life can be direct or indirect. Direct effects involve radiation interacting directly with biological materials like cells or prebiotic molecules. In contrast, indirect effects involve radiation interacting with the environment, particularly the atmosphere, influencing the potential emergence and development of life(Abrevaya, 2013).

Exploring the intricate relationship between radiation and habitability, we delve into the indirect effects radiation has on a planet's atmosphere. Currently, Earth's atmosphere acts as a protective shield against various forms of ionizing radiation from space. The interplay between radiation and the atmosphere, crucial for life as we know it, has evolved over time.

In the present-day scenario, our atmosphere effectively blocks high-energy photons like gamma- and X-rays. Oxygen (O_2) plays a role in absorbing short-wavelength UV (UVC), while ozone absorbs biologically damaging UVB between 200 and 350 nm (Diffey, 1991). However, in Earth's early stages marked by a different atmospheric composition, lacking ozone protection might have

resulted in "hazy" conditions that potentially altered the transmission of UV radiation (Wolf and Toon, 2010).

Shifting our focus to stellar X-rays, we uncover their significant impact on atmospheric evolution and the potential emergence of life. Theoretical models demonstrate how stellar X-rays can influence atmospheric components, releasing reactive species and catalyzing processes that affect the planetary environment. Additionally, the role of high-energy charged particles, such as cosmic rays, takes center stage in the context of biological evolution and the creation of habitable environments (Dartnell, 2011). Understanding these interactions sheds light on DNA damage, mutations, and the intricate processes that contribute to genetic variability and potential adaptation (Cromie et al., 2001).

Chapter 3

Water and Habitability

In this chapter we begin by unraveling the nature of water—its molecular makeup and its indispensable connection to life. Tracing its cosmic journey, we explore when and how water appeared in the universe, shaping the conditions for life as we recognize it on Earth. Exploring the landscape of exoplanets, focus our attention on the complications of water's existence and potential loss.At last, investigate how the presence or absence of water influences the habitability of these distant worlds, offering crucial insights into the broader canvas of life beyond our solar system.

3.1 Water existences

The profound and undeniable role of liquid water in the emergence, progression, and sustenance of life on Earth is widely acknowledged. Covering two-thirds of the Earth's surface, water plays a pivotal role as a vital resource for both plants and animals. The preservation of our planet's freshwater reservoirs becomes increasingly imperative as the global population continues to grow. Constituting 75% of the human body mass and standing as a primary component of organism fluids, water is a key compound essential for life on Earth. Hence, the principle "follow the water" serves as a guiding force in the realm of astrobiology (Irion, 2002).

Water exists in three states—liquid, vapor, and solid—on the Earth's surface under standard temperatures and pressures. Beyond our planet, water is pervasive in the universe, found in galaxies, stars, the Sun, planets, their satellites, ring systems, asteroids, and comets. The exceptional properties of water make it vital for life as we comprehend it on Earth. Firstly, it stands as the only substance abundant in liquid form at typical surface temperatures. Secondly, it excels as a solvent, facilitating the dissolution of various substances, promoting the transport of nutrients to cells, and aiding in waste elimination (Lynden-Bell et al., 2010).

3.1.1 What is water?

The stable molecule we know as water, composed of two hydrogen atoms and one oxygen atom, results from a highly exothermic chemical reaction. In this reaction, two hydrogen molecules (H_2) and one oxygen molecule (O_2) combine, producing water (H_2O) and releasing a substantial amount of energy (572 kJ/mol). Represented as H_2O, the molecular structure of water is triangular, with the apex being the oxygen atom and the two hydrogen atoms forming an angle of approximately 104.5°. Oxygen, with six valence electrons and the need for eight to complete its valence shell, shares two electrons from the hydrogen atoms. Due to differences in electron affinity, the molecule bends, causing the hydrogen atoms to appear on the same side. This bent structure classifies

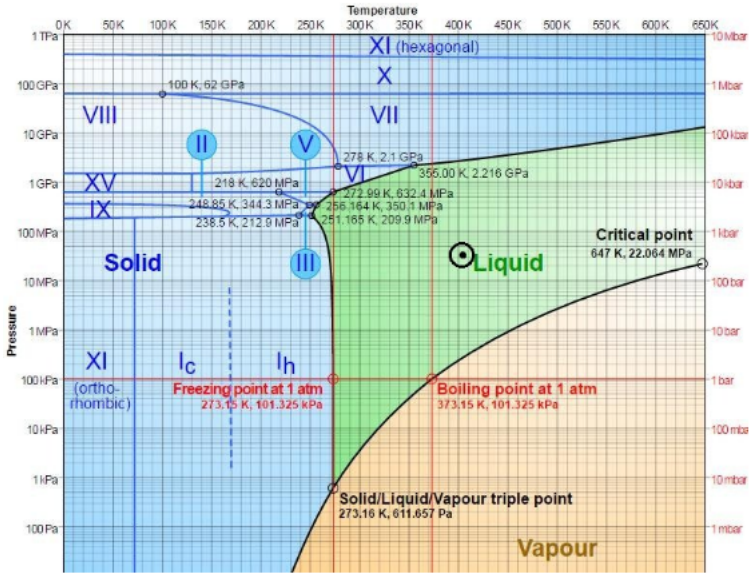

Figure 3.1: Behavior of different phases of water in different pressure and temperature(Rampelotto et al., 2018)

water as a polar molecule due to its polar covalent bonds and shape Rampelotto et al. (2018). Water's exceptional solvent properties, a result of its polarity, play a crucial role in its ability to interact with a variety of substances. The polarity of water, arising from its ability to induce temporary dipoles in nonpolar molecules, allows it to interact differently with charged and polar substances. When polar molecules interact with water molecules, which have partially positive and negative ends, a three-dimensional sphere of water molecules surrounds the solute. This unique property enables water to dissolve and accumulate a variety of substances essential for life. If the molecular bonds in water were linear instead of having the characteristic bent structure, its solvent capabilities might not be as strong, potentially influencing the conditions for the origin of life.

Crucial for the sustenance of life on Earth, water exhibits extraordinary properties, allowing it to naturally manifest in three distinct phases: gas, liquid, and solid. Key characteristics elucidated by Hanslmeier (2010) encompass:

Density Differences: Liquid water, often denser than its icy counterpart, forms a protective surface layer, vital for safeguarding life beneath it against freezing.

Neutral pH: Pure water maintains a neutral pH, marked at 7, indicating its neither acidic nor basic nature.

Boiling and Freezing Points: Under standard pressure, water boils at 100°C and freezes at 0°C. However, the boiling point is subject to environmental pressure, with higher pressures elevating the boiling point.

The water phase diagram determines phase boundaries contingent on temperature and pressure(Fig. 3.1). The triple point, where water concurrently exists in all three phases, occurs at 0.01°C (273.16 K) and 611.657 Pa pressure. In conditions of low pressure, such as on Mars, water boils at a higher temperature (approximately 38.5°C), posing challenges for the presence of liquid water on the Martian surface.

3.1.2 Water and Life

Defining life in astrobiology is a tricky task. Disagreements about when and how life began, along with the unclear line between living and nonliving things, make it complex. Whether viruses are considered life and the possibility of artificial life add more complexity.

Yet, in the middle of all this uncertainty, certain agreed-upon characteristics define living organisms. These include having an organized structure, with cells as the basic units of life, and engaging in metabolic processes (anabolism and catabolism) for survival. Living entities can regulate internal conditions to stay stable in changing environments (homeostasis), respond to environmental changes (response), undergo growth, reproduction, and adapt to their surroundings individually and as a population (evolution).(Rampelotto et al., 2018).

Considering life involves thinking about additional factors like being carbon-based and having genetic information stored as DNA. However, it's crucial to recognize that these traits together create a specific concept of life based on what we currently know. Imagining different life forms that might exist elsewhere in the universe is quite challenging. Therefore, current efforts mainly concentrate on finding known features of extraterrestrial bodies that could provide conditions suitable for supporting life as we currently understand it.

Water plays a crucial role in supporting life on Earth because of its remarkable properties. Its capacity to exist in all three phases contributes to a wide variety of climates, habitats, and intricate interactions between physical and chemical reactions. As a polar molecule, water excels as a solvent, dissolving many chemicals essential for metabolic reactions. Additionally, its dipole nature allows hydrophobic organic molecules, like lipids, to create cellular membranes. Although other solvents are imaginable, there is a consensus that water is a fundamental requirement for life. (Mottl et al., 2007). However, the existence of water does not assure the existence of life. Many uncertainties surround the probability of life emerging and evolving on a celestial body with water. Our understanding of how life began on Earth is limited. Did it come from an external source, or did Earth's formation and evolution create conditions for life to start here? The chemical reactions and environmental conditions essential for life's emergence on Earth are still actively debated. Currently, it's difficult to pinpoint all the circumstances that led to the birth of the first living cells on Earth. (Pascal et al., 2006).

Nevertheless, it remains indisputable that every recognized living entity is dependent on liquid water. Despite the widespread presence of water in the cosmos, liquid water remains conspicuously rare. The majority of water discovered on extraterrestrial entities manifests in either solid or gaseous states, with the potential exception of limited surface water on Mars. Pinpointing the exact temperature and pressure parameters conducive to liquid water on distant planets and moons continues to pose a formidable challenge. As a result, we have not conclusively pinpointed locations where life could potentially emerge and progress beyond Earth (Encrenaz and Mizon, 2007).

Despite the lack of concrete evidence of extraterrestrial life, the strength and adaptability of life across diverse environments on Earth, even in extremely challenging habitats, suggest that life may extend beyond our planet's boundaries. The discovery of extremophilic microbes has helped alleviate skepticism about the potential for extraterrestrial life.

Thriving in extreme conditions, extremophiles exemplify that life exists wherever liquid water is found on Earth. This has led to increased astrobiological interest within our solar system and beyond, fueled by recent discoveries like liquid water on Mars, potential subsurface liquid oceans on Europa and Enceladus, and the detection of organic molecules on Titan.

The quest for extraterrestrial life appears to be a question of time. As highlighted in this chapter, the crucial role of water in this pursuit takes center stage. The initial phases involve com-

prehending the origins and widespread occurrence of water in the universe, laying the groundwork for exploring life beyond our Earth. This exploration is poised to broaden our comprehension of the essence of living organisms in the expansive cosmos. The realization that we are not solitary entities is bound to permanently reshape humanity's self-perception.(Mottl et al., 2007).

3.1.3 When did water appear?

In the initial stages of the universe after the Big Bang, a dense and hot state underwent cooling as it expanded. This cooling process led to the creation of neutrons and protons. Subsequently, nucleosynthesis, the formation of light atomic nuclei such as hydrogen and helium, commenced. These elements played a vital role in the development of primordial stars. Initially, the universe was primarily composed of hydrogen (about 76%) and helium (about 24%). Over time, through the processes of stellar evolution and nuclear fusion, hydrogen underwent transformations into various elements, including oxygen.(Rampelotto et al., 2018).

Stars produce energy through mechanisms such as the proton-proton chain reaction and the carbon-nitrogen-oxygen (CNO) cycle, resulting in the generation of both energy and light chemical elements. Throughout their life cycles, stars undertake the synthesis of heavier elements, essential components for the formation of water. The fundamental role of stellar nucleosynthesis, responsible for creating elements within stars, becomes apparent in the generation of elements beyond hydrogen and helium.

Originating in interstellar clouds, water molecules were formed from the remnants of massive stars' end-of-life stages. In these final stages, substantial quantities of new nuclei were synthesized through nuclear reactions triggered by a flood of neutrons. These clouds comprise gases such as hydrogen and helium, along with heavier atoms and dust composed of various compounds, including water ice.

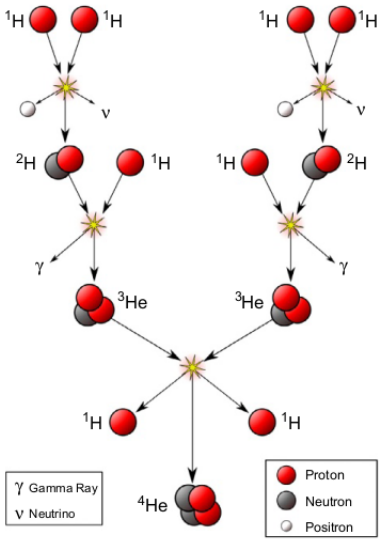

(a) Proton-proton chain reaction(Rampelotto et al., 2018)

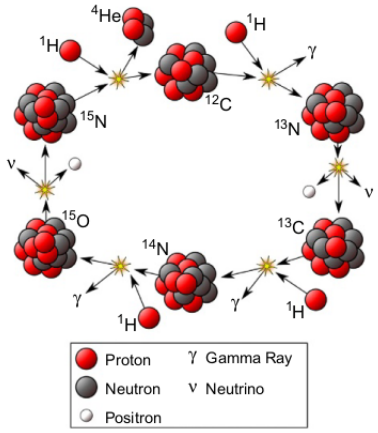

(b) CNO cycle reaction(Rampelotto et al., 2018)

3.1.4 Water and water loss in Exoplanets

Dominguez (2016) looked at how much water there is and how it's related to the metal content of stars in other planetary systems. They discovered that figuring out the H_2O/SiO_2 ratio in clouds with similar metal levels to our sun can help us understand the same ratio on Earth today. This supports the "wet" idea, which suggests that Earth might have gotten its water locally during its formation. Studies on how water forms in clouds with really low metal content indicate that these clouds could have a lot of water vapor. If one of these clouds collapsed into a disk that forms planets, some of this water vapor might have played a part in making the planets(Bialy et al., 2015).

The exploration of water vapor in the atmospheres of extrasolar planets has evolved over time. Ehrenreich et al. (2007) initiated attempts to detect water vapor on the HD189733b exoplanet using the Spitzer telescope. Although initial observations lacked the sensitivity to confirm water vapor, subsequent studies, as highlighted by (Rampelotto et al., 2018), have successfully identified water vapor in the atmospheres of various extrasolar planets, including HD 189733 b, HD 209458 b, Tau Boötis b, HAT-P-11b, XO-1b, WASP-12b, WASP-17b, and WASP-19b.

Employing an enhanced energy-limited escape model, Bolmont et al. (2017) calculated the quantity of water lost in their study. This model relies on two distinct types of spectral radiation: Far-Ultraviolet (FUV, 100–200 nm) for the photodissociation of water molecules and Extreme Ultraviolet (XUV, 0.1–100 nm) for heating the exosphere. It's noteworthy that, in their investigation, the planet is presumed to be in a circular orbit at the conclusion of the protoplanetary disk phase, resulting in a consistent orbit throughout its evolutionary process. The mass loss is given by"

$$\dot{m}\frac{dm}{dt} = \epsilon\frac{F_{\rm XUV}\pi R_{\rm p}^3}{\mathcal{G}M_{\rm p}(a/1{\rm AU})^2} \tag{3.1}$$

$$m = \epsilon\frac{\pi R_{\rm p}^3}{\mathcal{G}M_{\rm p}}\int_0^t \frac{F_{\rm XUV}}{(a/1{\rm au})^2}\,dt \tag{3.2}$$

where a is the planet's semi-major axis, $R_{\rm p}$ its radius and $M_{\rm p}$ its mass. ϵ denotes fraction of incoming energy converted into gravitational energy through mass loss.

Ribas et al. (2016) used the same way estimated ϵ considering 1D radiation hydrodynamic mass-loss simulations based on the calculations of Owen and Alvarez (2015). For incoming XUV fluxes ranging from 0.3 to 200ergs^{-1} cm^{-2}, the efficiency remains higher than 0.1 , however, for incoming XUV fluxes exceeding 200ergs^{-1} cm^{-2}, the efficiency decreases, reaching 0.01 at 10^5ergs^{-1} cm^{-2}. The parameter t_0 is defined as initial time specifically the moment when the protoplanetary disk dissipates. They considered that when the planet is within the disk, it is shielded and doesn't lose mass . Also they assumed that protoplanetary disks around dwarfs such as Proxima typically dissipate between $t_0 = 3$Myr and 10Myr.

Ribas et al. (2016) focused on the prevailing composition of the atmosphere, primarily consisting of hydrogen and oxygen. Utilizing the previously mentioned mass loss equation, they calculated the ratio of the oxygen escape flux to the hydrogen escape flux. This ratio, illustrating the connection between hydrogen and oxygen escape fluxes in the hydrodynamic outflow, aligns with prior researchHunten et al. (1987); Luger and Barnes (2015).

$$r_{\rm F} = \frac{F_{\rm O}}{F_{\rm H}} = \frac{X_{\rm O}}{X_{\rm H}}\frac{m_{\rm c} - m_{\rm O}}{m_{\rm c} - m_{\rm H}} \tag{3.3}$$

This ratio that related to the crossover mass $m_{\rm c}$ given by:

$$m_{\mathrm{c}} = m_{\mathrm{H}} + \frac{kTF_{\mathrm{H}}}{bgX_{\mathrm{H}}} \tag{3.4}$$

where T,g and b represent the exosphere's temperature,gravity of the planet and collision parameter between oxygen and hydrogen respectively. In the oxygen and hydrogen mixture, they considered $X_{\mathrm{O}} = 1/3, X_{\mathrm{H}} = 2/3$, which corresponds to the proportion of dissociated water.

This analysis entails computing the flux of hydrogen atoms, a process that necessitates estimations of the XUV luminosity of the relevant star and the temperature T. Bolmont et al. (2017) and Ribas et al. (2016) delved into this calculation, considering different XUV luminosities to estimate mass loss for Trappist-1 planets and Proxima b, respectively. Nevertheless, it is essential to note that the primary objective of this section is not to determine the specific quantity of water mass loss.

Chapter 4

Proxima b and TRAPPIST-1's planets

In this chapter, we explore the possibilities of life on two fascinating cosmic stages: Proxima b and the planets around TRAPPIST-1. We start by looking closely at Proxima b, investigating its chances for habitability. We delve into its initial water content, energy dynamics, and how its atmosphere and climate play a role. Shifting our gaze to the TRAPPIST-1 system, we explore the atmospheres of these distant planets and investigate the presence of water and seeking vital clues that illuminate the conditions for possible life.

4.1 Proxima b

Identification of a planet in orbit around Proxima Centauri, the nearest star to the Sun, by Anglada-Escudé et al. (2016) has turned the attention for extraterrestrial life on exoplanets to the vicinity of our solar system. Proxima Centauri b has a mass closely approximating that of Earth. Its orbit within a temperate zone raises the exciting prospect of discovering a habitable planet in our closest cosmic neighborhood. The detection of this planet resulted from a reanalysis of prior radial velocity measurements, providing the minimum mass (m sin i), where i represents the unknown orbital inclination angle. The minimum mass is reported between 1.10 and 1.46 Earth masses ($M_{\oplus}$)(Brugger et al., 2016).

Proxima b orbits around its host star in 11.2 days and has a semimajor axis distance of 0.05 AU. In contrast to many other discovered exoplanets, this short distance does not result in a high surface temperature for Proxima b. Proxima Centauri, as a red dwarf, emits only 0.15% of the Sun's luminosity, with an effective temperature of 3050 K. Consequently, a planet positioned at 0.05 AU from Proxima Centauri exhibits an equilibrium temperature of approximately 234 K (Anglada-Escudé et al., 2016). Assuming that Proxima b is surrounded by an atmosphere with a surface pressure of one bar, this temperature closely aligns with the melting point of water. This implication places the planet within the habitable zone of its host star(Brugger et al., 2016).

4.1.1 Potential Habitability

In the exploration of exoplanets, comprehensive evaluation of habitability requires detailed information about various properties, but technological limitations hinder obtaining such data, even for the nearest exoplanets. During the initial phase of searching for Earth-like planets, comparisons between deduced properties and expected characteristics of habitable worlds help assess the potential habitability of newly discovered exoplanets. The size of an exoplanet is a crucial initial indicator of its nature—whether it resembles a compact, rocky planet like Earth or displays

characteristics of a larger, volatile-rich mini-Neptune. Currently, our knowledge is limited to the minimum mass value for Proxima Centauri b. The 1.5% probability of aligned orbits producing visible transits from Earth offers a potential avenue for determining the exoplanet's actual mass and radius in the future. Until then, the assessment of Proxima Centauri b's likelihood of being a rocky planet relies on comparisons with a growing population of other exoplanets with more well-known properties(Anglada-Escudé et al., 2016).

4.1.2 Initial water content on Proxima b

Understanding the original water content of Proxima b, tracking its water loss over time, and determining its current water state are critical factors in evaluating the potential habitability of the exoplanet. However, even Earth's water content has not been precisely determined. Earth's surface water is estimated to be around 1.5×10^{24} g, equivalent to one "ocean" of water. The quantity of water within Earth's interior, especially in the mantle, remains uncertain, with estimates ranging from 0.3 to 10 times the volume of Earth's oceans. Notably, it is widely believed that Earth's core does not contain a significant amount of hydrogen(Ribas et al., 2016). In considering the potential growth of the Proxima system, similar to the formation of our terrestrial planets, there are indications suggesting that Proxima b might be less moist compared to Earth.

First, relationship between the snow line, habitable zones, and water delivery in protoplanetary disks, specifically exploring their implications for exoplanet Proxima b. The snow line, where volatile materials like water can exist in solid form, tends to be farther from the habitable zone around low-mass stars. While Proxima Centauri's habitable zone is closer to the star than the Sun's, the snow line may have been at a similar distance, suggesting less efficient water delivery to Proxima b at larger dynamical separations (Raymond et al., 2004). Protoplanetary disks, the birthplaces of planets, are not static. As they cool and lose mass over time, the snow line shifts inward. Early models of the Sun propose that the Solar System's snow line could have been as close as one astronomical unit (AU) at certain times, but the region up to 2.7 AU lacks water, possibly due to the influence of Jupiter during its formation(Ribas et al., 2016). The likelihood of Proxima Centauri hosting a gas giant within a few astronomical units is low, and even at greater distances, the gravitational influence of such a planet would likely be detectable. However, limitations in detection methods, particularly the Doppler method, leave a possibility that a large, face-on orbiting planet might go unnoticed. Ribas et al. (2016) estimated a low probability of concealing a gas giant within 10 astronomical units of Proxima Centauri, even if confirmed in the future. The existence of such a planet could significantly impact Proxima b's atmosphere and overall state, introducing non-zero eccentricity and tidal effects. Yet, due to limited information and speculative nature, considering additional planets is currently deemed unnecessary.

Proxima b's potential loss of atmosphere and oceans can be attributed to a second factor: the higher energy levels involved in its formation compared to Earth's formation. The collision speed between orbiting objects, a critical aspect in planet formation, is intricately linked to local velocity dispersion and the mutual escape speed of the bodies involved. The random velocities of a planet within the habitable zone are explicitly tied to the local orbital speed, represented as $\sim (M_*/r_{HZ})^{1/2}$, where M_* represents the stellar mass (Lissauer, 2007). In the case of Proxima, the impacts contributing to the formation of planets within the habitable zone were, on average, several times more energetic than those shaping Earth. This heightened energy during Proxima b's formation potentially resulted in a significant loss of its atmosphere and potential oceans. The increased collision energy levels likely played a crucial role in shaping the distinct atmospheric and oceanic conditions of Proxima b compared to Earth.

The third factor suggesting a more rapid formation of Proxima b compared to Earth involves several considerations. Assuming a sufficiently high surface density conducive to the formation of an Earth-mass planet, both simple scaling laws and N-body simulations indicate that planets within the habitable zones of stars with around 0.1 $M_\odot$ can emerge within 0.1 to a few million years. Even if Proxima b formed swiftly, the dissipation of the gaseous disk within a few million years could have triggered a brief yet intense phase of giant collisions. This concentrated impact energy over a shorter period than Earth's formation may have contributed to increased water loss. Simulation studies propose that in-situ growth can transport water-rich material to the habitable zones of low-mass stars. However, these simulations, while informative, did not specifically target very low-mass stars like Proxima. It's anticipated that the water-depleting effects discussed earlier become more pronounced for the lowest-mass stars, leaving the retention of water uncertain.

Additionally, there's a significant possibility that Proxima b initially formed at a greater distance from the star and subsequently migrated inward. Migration is plausible for planetary bodies with masses exceeding approximately 0.1–1 $M_\otimes$ due to tidal interactions with the protoplanetary disk, and since Proxima b falls within this mass range, migration emerges as a feasible scenario (Ribas et al., 2016).

The presence of "hot super-Earths" in the planetary population could be accounted for by the development of planetary embryos at various astronomical units (AU), moving towards the inner edge of the protoplanetary disk and experiencing a subsequent phase of late collisions. If Proxima b or its constituent elements have originated farther from the star and migrated inward, their compositions might deviate from the local disk conditions, potentially containing a significant amount of water. If migration did occur, it probably occurred in the early gaseous disk phase, impacting the planet's initial water content while leaving its irradiation or tidal evolution unaffected.

Various mechanisms could have influenced the water content of Proxima b throughout its formation. If Proxima's protoplanetary disk underwent external photoevaporation, the snow line may have been positioned far from the star, potentially inhibiting the delivery of water to Proxima b. Additionally, the short-lived radionuclide 26 Al is considered to play a crucial role in determining the thermal structure and water contents of planetesimals, especially those that accrete rapidly, a scenario that might apply to Proxima b's building blocks. Another possibility considered is a late bombardment of water-rich material on Proxima b, although for this to deliver an ocean's worth of water, it would need to be significantly more abundant (1–2 orders of magnitude) than the late heavy bombardment experienced by the Solar System. However, the exact amount of water delivered or retained remains uncertain. Proxima b's water budget might range from having an Earth-like water content that received slightly more water but lost a higher fraction to scenarios such as an ocean-covered planet with building blocks condensing beyond the snow line or a dry world where surface water was removed by impacts and early heating(Ribas et al., 2016).

4.1.3 Energy

The effective stellar flux (S_{eff}), which representing the amount of energy a planet receives from its host star, is a crucial factor in determining a planet's potential habitability. Kopparapu et al. (2013) established the limits of the habitable zone (HZ) through comprehensive climate and geophysical modeling. The outer boundary of the HZ was conservatively defined as the maximum greenhouse limit of a CO_2-rich atmosphere, beyond which additional CO_2 would not further increase the planet's surface temperature. For Proxima Centauri, a star with a surface temperature of 3050 K, this outer limit of the HZ corresponds to an S_{eff} of 0.23 times that of Earth, translating to a mean orbital radius of 0.081 AU. Similarly, the inner boundary of the HZ was conservatively determined

by the runaway greenhouse limit, a point where a planet's temperature would escalate, leading to the loss of all its water. In the case of an Earth-sized planet orbiting Proxima Centauri, this inner limit corresponds to an S_{eff} of 0.92 or a distance of 0.041 AU. These boundaries provide crucial benchmarks for assessing the potential habitability of planets in the Proxima Centauri system.

The consideration of stellar ultraviolet radiation (UVR) alongside stellar flux is a crucial aspect of evaluating planetary habitability, especially in the context of exploring the potential for life beyond Earth. Instrumental in assessing a planet's capacity to support surface life, modeling studies on stellar UVR play a significant role. Nevertheless, certain studies in this domain may introduce inaccuracies, such as neglecting a planetary atmosphere or employing unrealistic atmospheric compositions. This can result in imprecise estimations of the UV flux that reaches the planet's surface.Moreover, the assessment of the biological impact of UV often relies on extrapolations from empirical data, such as UV biological action spectra (UV-BAS) or UV 'lethal dose' (UV-LD). Limitations arise from low fluence rates that do not align with realistic astrophysical scenarios. These extrapolations also have a tendency to overlook variations in microorganism survival linked to growth stage and physiological conditions, potentially introducing biases in predicting the effects of radiation on life in specific planetary environments. For instance, a laboratory assay demonstrated an increase in microorganism biomass when exposed to UVC fluences comparable to weak flares. However, caution is necessary when applying such results due to the artificial physiological conditions and the protective effects of the culture medium considered in the experiments. In essence, both stellar flux and UVR are essential considerations when evaluating a planet's potential habitability. A comprehensive and cautious approach is imperative to understand the intricate interplay of these factors. (Abrevaya, 2013).

In their study, Abrevaya (2013) investigated the varying absorption of UV flux (200–380 nm) under different atmospheric scenarios to assess the impact of different atmospheric compositions and pressures on the stellar ultraviolet radiation (UVR) reaching the surface of Proxima b. Their findings revealed that UVR on Proxima b is primarily dominated by the UVA range (315–400 nm), contributing 92 percent of the incident radiation. The UVA flux without atmospheric attenuation was measured at 1.08 Wm^{-2}, a considerably lower value than the UVA flux on Earth's surface (e.g., 30–50 W m^{-2} for clear sky). Even under the attenuation of considered atmospheres, the UVA flux on Proxima b's surface would not preclude the possibility of supporting 'life as we know it.' The efficacy of UVA in inducing lethal damage depends on mechanisms that, in the presence of oxygen, generate reactive oxygen species. However, studies indicate that O-rich atmospheres are not anticipated to exist on planets orbiting M-type stars, potentially reducing the damage induced by UVA in this context. Regarding the UVB (280–315 nm) and UVC (200–280 nm) bands, atmospheric absorption is projected to increase with higher CO_2 content and atmospheric pressure, regardless of atmospheric compositions. Significant reduction in flux in these bands is expected for CO_2 contents exceeding 50 percent and atmospheric pressures surpassing 2000 mbar. This is crucial as UVB and UVC radiations, absorbed by nucleic acids, may undergo chemical modifications, leading to the loss of their biological functions upon exposure. Despite this, the stellar UVB fluence rate reaching Proxima b's surface (0.026 W m^{-2}) is lower than that on Earth (around 2 Wm^{-2}), suggesting that microorganisms could potentially survive even without the protective effect of an atmosphere. In the case of UVC, the terrestrial atmosphere blocks this wavelength range, making it challenging to use data from experiments involving solar radiation on Earth's surface as a reference for assessing the impact of UVC on Proxima b. The available data on the biological effects of solar UVC on microorganisms in space comes from experiments conducted in low Earth orbit, where certain microorganisms, including cells of Chroococcidiopsis and spores of Aspergillus sydowii and Aspergillus versicolor, exhibited survival after 1.5 years of

exposure. Additionally, viable spores of Bacillus subtillis were recovered after 6 years of exposure to solar UVR in space.

Abrevaya (2013) computed the solar UVC fluence rate at the top of the atmosphere, revealing a value of 6.27 W m^{-2} — notably 95 times higher than the estimated UVC flux at the surface of Proxima b (0.066 W m^{-2} without atmospheric protection). This substantial difference suggests the potential for 'life as we know it' to thrive on Proxima b's surface, particularly considering the anticipated low UVC irradiation levels during quiescent stellar conditions. Furthermore, the consideration of atmospheric attenuation introduces the possibility that specific atmospheric compositions and pressures could provide additional protection against harmful UV wavelengths, challenging the notion that only O-rich Earth-like atmospheres offer such protection. However, the study acknowledges that, even in the absence of an atmosphere, the UV fluence rates on Proxima b's surface during stellar quiescence are likely to have negligible effects on life.

Additionally, Battistuzzi et al. (2023) have demonstrated that Proxima Centauri b receives an irradiance of approximately 64 μmol m^{-2} s^{-1} in the visible spectrum, accounting for roughly 3% of Earth's solar irradiance. This substantial amount of light surpasses the requirements for the survival and growth of certain land plants and cyanobacteria by over 20 and 180 times, respectively. Moreover, a model based on this stellar environment suggests that organisms on Proxima Centauri b would be light-limited but still exhibit gross productivities exceeding those observed in many terrestrial grasslands and the open ocean on Earth.

4.1.4 Atmosphere and Climate

In the absence of an atmosphere, the entire incoming stellar flux is absorbed and re-emitted on the planet's day-side as a black body. Conversely, if there is an atmosphere, it has the capacity to transport heat to the night side. By integrating comprehensive observation initiatives conducted both from ground-based and space platforms, it becomes feasible to quantify accurately the portion of incident flux redistributed to the planet's night side. If there is no discernible redistribution, it may suggest the planet lacks an atmosphere, making it less likely to support life. On the other hand, the identification of substantial energy transport would imply the presence of an atmosphere or ocean facilitating energy transfer. In such a scenario, Proxima b would emerge as a considerably more intriguing candidate for habitability. In either scenario, these observations represent a significant leap forward in our comprehension of terrestrial worlds beyond our Solar System(Ribas et al., 2016). Turbet et al. (2017) was one who described the results of climate models specifically for Proxima Centauri b. Utilizing a 3D global climate model, they simulated the atmospheric and water cycle of the newly discovered exoplanet, accounting for its two probable spin states. During this simulation, they varied the planet's presently unknown surface water inventory and the concentration of CO_2 greenhouse gas in its assumed $N_2 - CO_2$ atmosphere—a prevalent atmospheric composition shared by more giant rocky planets in our solar system, including Earth in its early stages.

Several potential climate scenarios which were identified by Turbet et al. (2017), suggested that Proxima Centauri b has the capability to sustain liquid water on its surface across a broad spectrum of conditions. The specific climate regime exhibited by Proxima Centauri b would be contingent upon its water inventory and the concentration of CO_2 in its atmosphere. Although the 3D global climate model explored by Turbet et al. (2017) did not incorporate feedback from mechanisms like the carbonate-silicate cycle, which plays a role in regulating atmospheric CO_2 levels, such mechanisms could contribute to maintaining temperatures above freezing. Consequently, the results from the 3D global climate model provide support for the notion that Proxima Centauri b

is, at the very least, potentially habitable.

4.2 TRAPPIST-1

The TRAPPIST-1 system consists of seven transiting planets. The three planets within the TRAPPIST-1 system (Gillon et al., 2016)are Earth-sized 4.1and indicate a likely rocky composition (Weiss and Marcy, 2014; Rogers, 2015). The host star, TRAPPIST-1, is a relatively small M8-type dwarf, comparable in size to Jupiter. This small host star enhances the possibility of detecting spectral signatures from the planets' atmospheres during their transits. The planets in the TRAPPIST-1 system orbit closely to their star, resulting in rapid completion of their orbits. This close-knit configuration facilitates more frequent transit observations, generating a greater volume of data within a given timeframe compared to planets with lengthier orbital periods. These factors make TRAPPIST-1 an optimal system for studying multiple Earth-sized rocky exoplanets in a similar environment, with some residing in the habitable zone of the systemLim et al. (2023).

However, TRAPPIST-1, classified as an ultracool dwarf star, likely persisted in the pre-main-sequence phase for hundreds of millions of years. Throughout this pre-main-sequence phase, the planets in the TRAPPIST-1 system were subjected to high-energy radiation emitted by the star, intensifying atmospheric escape processes. This impact was further emphasized by the planets' close proximity to the host star, as evidenced in studies conducted byWordsworth and Pierrehumbert (2014); Luger et al. (2015); Roettenbacher and Kane (2017).

Interestingly, TRAPPIST-1 continues to emit X-rays at a luminosity level comparable to that of the Sun, a noteworthy observation considering its smaller overall bolometric luminosity, documented by Wheatley et al. (2017). The cumulative extreme-ultraviolet energy received by the TRAPPIST-1 planets throughout their lifespan varies across specific planets, ranging from 10 to 1000 times the energy received by Earth, as outlined in studies by Fleming et al. (2020) and Birky et al. (2021). Flares on TRAPPIST-1, detected during the K2 mission, manifested at frequencies of approximately 0.02–0.5 per day, with each event releasing energy within the range of 10^{30} to 10^{33} erg (Vida et al., 2017).

4.2.1 Atmosphere

The James Webb Space Telescope is anticipated to analyze the atmospheres of TRAPPIST-1 planets, with the potential to identify gases such as CO_2 , CO, H_2O, CH_4 , or abiotic O_2 resulting from water photodissociation and subsequent hydrogen escape(Krissansen-Totton and Fortney, 2022).

The challenge lies in predicting if the TRAPPIST-1 planets have cultivated and maintained oxygen-rich atmospheres due to extensive hydrogen loss. On the inner planets (1b and c), the accrual of oxygen hinges primarily on the initial water availability and the efficacy of dry crustal sinks. The modern atmosphere on the inner planets 1b and c harbors detectable oxygen (¿ 1 bar) for about half the time. Conversely, the outer planets (1e, f, and g) exhibit a lower likelihood of abiotic oxygen accumulation. For these outer planets, atmospheric oxygenation is shaped not solely by the initial water inventory but also by atmospheric escape dynamics, the initial mantle redox state, and the effectiveness of various other crustal oxygen sinks, including water–rock reactions and extrusive lava oxidation. Increasing orbital separation leads to a diminishing probability of having oxygen-rich modern atmospheres, yet the complexity of influential factors suggests that explaining observed patterns of atmospheric oxygenation is not straightforward. The challenge of

predicting the presence or absence of significant atmospheres is considerable, particularly in the absence of more refined models for atmospheric nitrogen and nonthermal escape processes. In a broad sense, one would anticipate the lack of a substantial atmosphere on the inner planets. This expectation arises because, among the PACMAN model iterations consistent with observed mass–radius constraints, only about half maintain a dense atmosphere after 8 Gyr. On the outer planets, complete atmospheric erosion is considerably less likely, given the limited lifetimes of easily eroded runaway greenhouse atmospheres. Moreover, mass–radius constraints do not impose restrictions on condensed surface volatile reservoirs, enabling more model iterations with substantial atmospheres aligned with observed densities. Should the TRAPPIST planets indeed harbor significant atmospheres, they are likely to be dominated either by CO_2 or CO_2 –O_2 (or CO–O_2 if there is substantial photochemical dissociation of CO_2). While the possibility of atmospheres rich in water vapor cannot be entirely dismissed for the inner planets, the minimal insolation received by the outer planets indicates the likely absence or undetectability of atmospheric water vapor in transit spectra. The quantity of atmospheric CO2 in contemporary atmospheres is primarily influenced by initial endowments, escape physics (for the inner planets), and carbon cycle feedback (for the outer planets). However, the PACMAN model incorporates various simplifications that may lead to inaccurate predictions. The omission of primary atmospheres, the lack of explicit consideration of photochemistry, simplified escape parameterizations, and the limitation of volatile cycling to C-, H-, and O-bearing species are potential sources of concern. Nevertheless, any discrepancies between the outlined predictions and forthcoming observations from the James Webb Space Telescope (JWST) will serve as a catalyst for future model refinement and enhanced theoretical comprehension(Krissansen-Totton and Fortney, 2022).

4.2.2 Water

Considering an unfavorable scenario where water molecules undergo complete dissociation and accounting for various X-ray luminosity values of ultra-cool dwarfs (UCDs), specific regions in the parameter space were identified (Bolmont et al., 2017)where planets lose only a minimal amount of hydrogen (equivalent to the hydrogen reservoir in one Earth ocean) before reaching the habitable zone (HZ). In these regions, planets can also remain in the HZ for an extended duration. Upon entering the HZ, the remaining hydrogen has the potential to recombine with the remaining oxygen, forming water molecules that may subsequently condense. The prolonged stay of a planet in the HZ allows more time for the possible emergence and evolution of life, increasing the probability of observability.

Bolmont et al. (2017) suggested a potentially favorable zone for life around ultra-cool dwarfs (UCDs). Planets situated at orbital distances between 0.01 and 0.04 AU and orbiting brown dwarfs(BDs) with masses ranging from approximately 0.04 to 0.08 solar masses($M_\odot$), assuming an X-ray luminosity (L_X/L_{bol}) of 10^{-5} or $L_X = 10^{25.4}$ erg s^{-1} experience minimal hydrogen loss (less than 1 Earth ocean worth) during runaway greenhouse phases and subsequently have the potential for prolonged habitation in the habitable zone (HZ) – at least 1 billion years (Bolmont et al., 2012). If a higher X-ray luminosity ($L_X/L_{bol} = 10^{-4.5}$ or $L_X = 10^{26}$ erg s^{-1}) is considered, this favorable zone shifts toward higher orbital distances and greater UCD masses. In this scenario, planets orbiting UCDs with masses around 0.06 to 0.08 $M_\odot$ and situated between 0.02 and 0.04 AU lose less than 1 Earth ocean worth of hydrogen during runaway phases and subsequently enjoy extended periods in the HZ. However, the actual sweet spot for life could vary if the considered mechanisms do not occur or if the real XUV flux of BDs is lower than the upper value.

Despite uncertainties regarding escape mechanisms, especially regarding the joint escape of

Planet	Semi axis(AU)	Mass(M_{Jup})	Period(day)	Radius(R_{Jup})
Proxima b	0.04856	*	11.1868	**
TRAPPIST-1 b	0.01154	0.004323	1.510826	0.09956
TRAPPIST-1 c	0.01580	0.004115	2.421937	0.09787
TRAPPIST-1 d	0.02227	0.00122	4.049219	0.0703
TRAPPIST-1 e	0.02925	0.00218	6.101013	0.0821
TRAPPIST-1 f	0.03849	0.003269	9.207540	0.09323
TRAPPIST-1 g	0.06189	0.00103	18.772866	0.0674

Table 4.1: characteristics of Proxima b and Planets of TRAPPIST-1

hydrogen and oxygen, there exists a possibility that planets orbiting ultra-cool dwarfs (UCDs) could reach the habitable zone (HZ) with a significant water reservoir, even without requiring an initial water reservoir larger than Earth(Bolmont et al., 2017). This potential is further enhanced if the loss of hydrogen is limited by photolysis, specifically if the efficiency of this process is below 20 percent. Additionally, planets in the HZs of brown dwarfs (BDs) might be readily detectable in transit due to their substantial transit depths and short orbital periods, particularly for sufficiently bright sources (Belu et al., 2013; Triaud et al., 2013). With their large abundance in the Solar neighborhood, such planets could represent some of the best nearby targets for atmospheric characterization using the James Webb Space Telescope (JWST). Notably, the planets of the TRAPPIST system offer an ideal laboratory for testing mass-loss mechanisms.

Chapter 5

Time interval for Planets before entering Habitable Zone

This chapter presents a comparative analysis of habitable exoplanets orbiting M stars. The analysis focuses on identifying exoplanets with a mass less than 10 times that of Earth, which orbit M stars, and reside within the habitable zone. The aim of this study is to contribute to our understanding of potentially habitable exoplanets and their suitability for supporting life.

5.1 Target Exoplanets

The analysis was conducted by utilizing two datasets: one containing information on all known exoplanets (`http://exoplanet.eu/catalog/`) and the other specifically focused on habitable exoplanets (`http://www.hzgallery.org/table.html`). The Python programming language was employed to extract and filter the relevant data. First, exoplanets with a mass less than 10 Earth masses, orbiting M stars were identified from the database at `http://exoplanet.eu/catalog/`. Then, from `http://www.hzgallery.org/table.html`, those exoplanets which are in the habitable zone were obtained. Additionally, one more restriction was considered for this work, based on their t_{HZO} (The percentage of time during the orbital phase that a celestial body resides within the Optimistic Habitable Zone), requiring this value to be 100% (Table5.1).

Star name	SP-type	$M/M_{\odot *}$	Age_*(Gyr)	$T_{eff*}(K)$	Planet	Orbital period(day)	Ecc	a(AU)
GJ1002	M5.5V	0.12		3024	b	10.3465		0.0457
GJ1002	M5.5V	0.12		3024	c	20.202		0.0738
GJ 180	M2V	0.43		3371	c	24.329	0.09	0.129
GJ 273	M3.5	0.29		3382	b	18.64	0.1	0.0911
GJ 3293	M2.5	0.42		3466	d	48.1345	0.12	0.19394
GJ 357	M2.5 V	0.342		3505	d	55.698	0.033	0.204
GJ 667 C	M1.5V	0.33	2	3600	c	28.14	0.02	0.125
GJ 667 C	M1.5V	0.33	2	3600	e	62.24	0.02	0.213
GJ 667 C	M1.5V	0.33	2	3600	f	39.026	0.03	0.156
GJ 682	M3.5V	0.27		3028	b	17.478	0.08	0.08
K2-9	M2.5 V	0.3	1	3390	b	18.4498		0.091
Kepler-1649	M5V	0.2		3240	c	19.53527		0.0649
Kepler-1652	M2V	0.4	3.2	3638	b	38.09722		0.1654
Kepler-186	M1	0.54	4	3755	f	12909441	0.04	0.432
Kepler-296	M2 V	0.5		3740	f	63.33627	0.33	0.255
Kepler-309	M0 V			4713	c	105.356383		0.401
LHS 1140	M4.5	0.146	5	3131	b	24.736	0.06	0.0957
Prox.Cen	M5.5V	0.12	4.85	3050	b	11.1881	0.02	0.04856
TOI-1227	M4.5V	0.17	0.011	3072	b	2736397		0.0886
TOI-700	M2V	0.416	1.5	3480	d	37.42396	0.042	0.1633
TOI-700	M2V	0.416	1.5	3480	e	27.80978	0.059	0.134
TRAPPIST-1	M8	0.08	7.6	2560	d	4.04961	0	0.02227
TRAPPIST-1	M8	0.08	7.6	2560	e	6.099615	0	0.02925
TRAPPIST-1	M8	0.08	7.6	2560	f	9.20669	0	0.03849
TRAPPIST-1	M8	0.08	7.6	2560	g	12.35294	0	0.04683
GJ10393 [a]	M7.0V	0.089	8		b	4.91	0	0.0252
GJ10393	M7.0V	0.089	8		c	11.409	0	0.0443
Wolf 1069	M5.0 V	0.167		3158	b	15.564		0.0672

Table 5.1: Target planets with their main characteristics

[a]GJ10393 is the other name for Teegardens' Star

Therefore, the selected exoplanets meet the criteria for potential habitability as they are not only in the habitable zone but also spend the entire orbital phase within the Optimistic Habitable Zone. This suggests that these exoplanets may have conditions favorable for supporting life, including the potential existence of liquid water.

5.2 Evolutionary Models

In the exploration of planetary habitability, it becomes crucial to consider the temporal evolution of the habitable zone. While this aspect is often overlooked in studies focusing on planetary habitability, recent evidence sheds light on the dynamic nature of the habitable zone. The limits of the habitable zone closely mirror the evolution of host-star parameters, an insight drawn from the field of stellar evolution. During specific phases of a host star's life, the habitable zone can undergo rapid changes, potentially causing a planet observed within it at a given time to exit within a few million years((Gallet et al., 2017)).

This perspective introduces the concept of continuously habitable zone limits, emphasizing the time required for a planet within the habitable zone to foster the emergence of complex organisms. The minimum time needed for life to reach complexity remains uncertain and is often assumed within a range of 2 to 4 billion years, mirroring Earth-like conditions.

In this work, the adoption of an evolutionary model is underpinned by a holistic understanding of stellar evolution. The consideration of recent findings indicating simultaneous planet formation alongside host stars further informs this choice. Stellar evolution, encompassing the transformation of stars over time, shows duration variations based on mass, ranging from a few million years for the most massive stars to trillions of years for the least massive ones. These insights suggest a swift initial development of star–planet systems, aligning seamlessly with the rationale for employing an evolutionary model in conducting a comprehensive analysis."

5.2.1 Evolutionary Model of Baraffe 2015

In 1998, a set of evolutionary models for low-mass stars was introduced by Baraffe et al. (1998), utilizing the NextGen atmosphere models(Hauschildt et al., 1999). These models marked a significant advancement, ushering in a new era of consistent coupling between interior and atmosphere structures. Widely embraced for their capability to accurately reproduce various observational constraints, including mass-luminosity and mass-radius relationships, as well as color-magnitude diagrams, these models gained popularity. However, it's worth noting that the models exhibited notable shortcomings, such as predicting optical $(V - I)$ colors that were excessively blue for a given magnitude. After extensive efforts to address these deficiencies, the persistence has yielded positive results with the introduction of a new set of models Baraffe et al. (2015), surpassing the BCAH98 models. Evolutionary calculations rely on the same underlying physics to depict stellar and substellar interior structures. The primary modifications pertain to the atmosphere models, which establish the outer boundary conditions for the interior structure computation, as well as determine the colors and magnitudes for a given star mass at any specific age. Notable revisions have been implemented since the utilization of NextGen atmosphere models in the BCAH98 evolutionary models(Baraffe et al., 1998). Baraffe et al. (2015) considered evolutionary models for pre-main-sequence and main-sequence stars with masses ranging from 0.07 $M\odot$ to 1.4 $M\odot$. this model used the composition of the Sun, with some adjustments to the abundance of certain elements. The adjustments were made based on the CIFIST project, leading to slightly higher levels

of carbon, nitrogen, and oxygen, and an overall increase in the total heavy element content. The adopted helium abundance in the atmosphere models reflects the initial helium content of the Sun.

5.2.2 Evolutionary Model of Somers 2020

The repository contains a set of theoretical stellar evolutionary tracks and isochrones known as the Stellar Parameters of Tracks with Starspots (SPOTS) grid Somers et al. (2020). The calculations were performed using the Yale Rotating Evolution Code, incorporating updates that include a treatment of surface starspots. The primary aim of this suite of evolutionary models is to offer the scientific community up-to-date predictions on how starspots and magnetic activity influence the structure of stars. This model is a set of stellar evolution tracks and isochrones that consider the impact of surface activity and starspots. It accounts for the inhibition of convective energy transport caused by magnetic field lines near the surface and the influence of cool surface regions on photosphere boundary conditions.

5.3 Luminosity versus Age

In the initial part of this section, with considering mass of HZ exoplanet(less than 10 Earth mass) and the spectral type of their host stars (M Type), a list of target stars and their planets was compiled(Table5.1). Subsequently, the masses of the host stars associated with the identified planetary systems were determined from this list. To delve into the stellar evolution of these target stars, two distinct evolutionary models were employed (Baraffe et al., 2015; Somers et al., 2020). Evolutionary model of Somers et al. (2020) contains various fractions of star spots, but the point is when applying the various fractions of this model, we did not notice so significant differences in luminosity for our purposes (Fig5.1). So, we used the f=0 for the rest of this work, as it has demonstrated the highest luminosity.

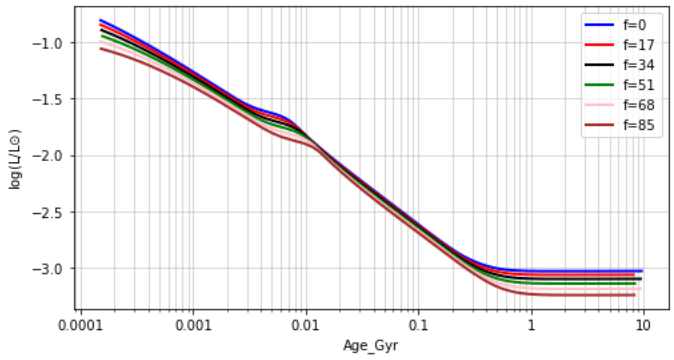

Figure 5.1: evolution of the luminosity for stars with masses equal to 0.1 M$\odot$ for different fraction of star spot from the model of Garrett 2019

Fig. 5.1 shows the evolution of bolometric luminosity for stars with M=M$_\odot$. Different colors represent different fraction of star's spot (f=0%, f=17%, f=34%, f=51%, f=68% and f=85%). However, there is an obvious difference between different spot fractions. We will consider non-spot stars (f=0) as the harshest situation, unless situations come up where f=0 gives an unexpected outcome, necessitating consideration of other fractions.

We reconstructed the Luminosity-age plot of what Ribas et al. (2016) did and compare it with the Somers et al. (2020)(Fig 5.2).

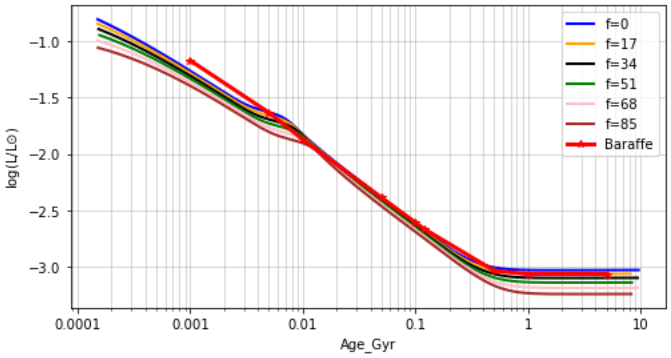

Figure 5.2: comparing star evolutionary between models of Baraffe et al. (2015) & Somers et al. (2020) for star mass = 0.1 M⊙ ,

As seen in Figure5.2, both Baraffe (the red * line) and Somers' (different colorse for different spot fractions)evolutionary models of luminosity exhibit similar results which is acceptable for our work. Therefore, we can use both models for our objective. The reason for employing two models is to accommodate different masses of stars; some are present in the Baraffe model, while others are in the Somers model. For the masses that overlap in both models, we incorporate data from both in our plots.

In the next step, we found out the masses of the host stars for the target planets from the data we had. From those two models(Somers et al., 2020; Baraffe et al., 2015), we constructed luminosity-age evolutionary plots (for nineteen stars) as well as present-day luminosity plots for each stellar mass. These plots offer valuable insights into the temporal evolution of the selected stars and serve as a foundational component for the subsequent analyses and interpretations in this study(Figs5.3, 5.4, 5.5).

In all these plots, Red line represents the models of Roettenbacher and Kane (2017), the blue line shows the modelSomers et al. (2020) with 0% spot fraction, black line explains the modelSomers et al. (2020) with 34% spot fraction. light blue Horizontal represents the present-day bolometric luminosity of star. Horizontal dark blue, red and green explain the minimum luminosity that each star could have to place in habitable zone.

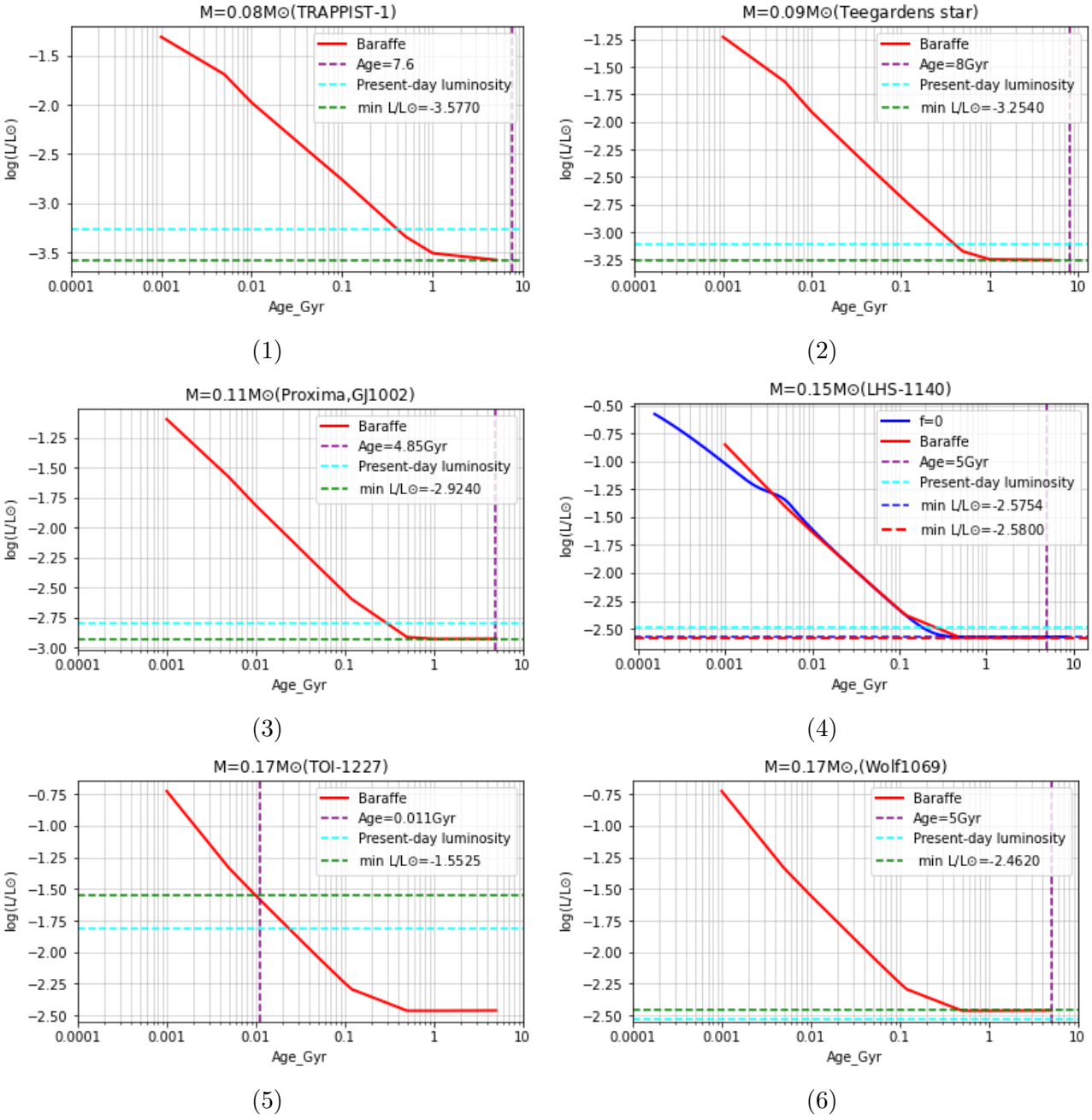

Figure 5.3: Evolution of Luminosity and preset-day bolometric luminosity for stars with masses from $0.08M_{\odot}$ to $0.17M_{\odot}$, considering two different evolutionary models (Baraffe et al., 2015; Somers et al., 2020).For model of Somers et al. (2020) we considered only the spot fraction equal to zero.

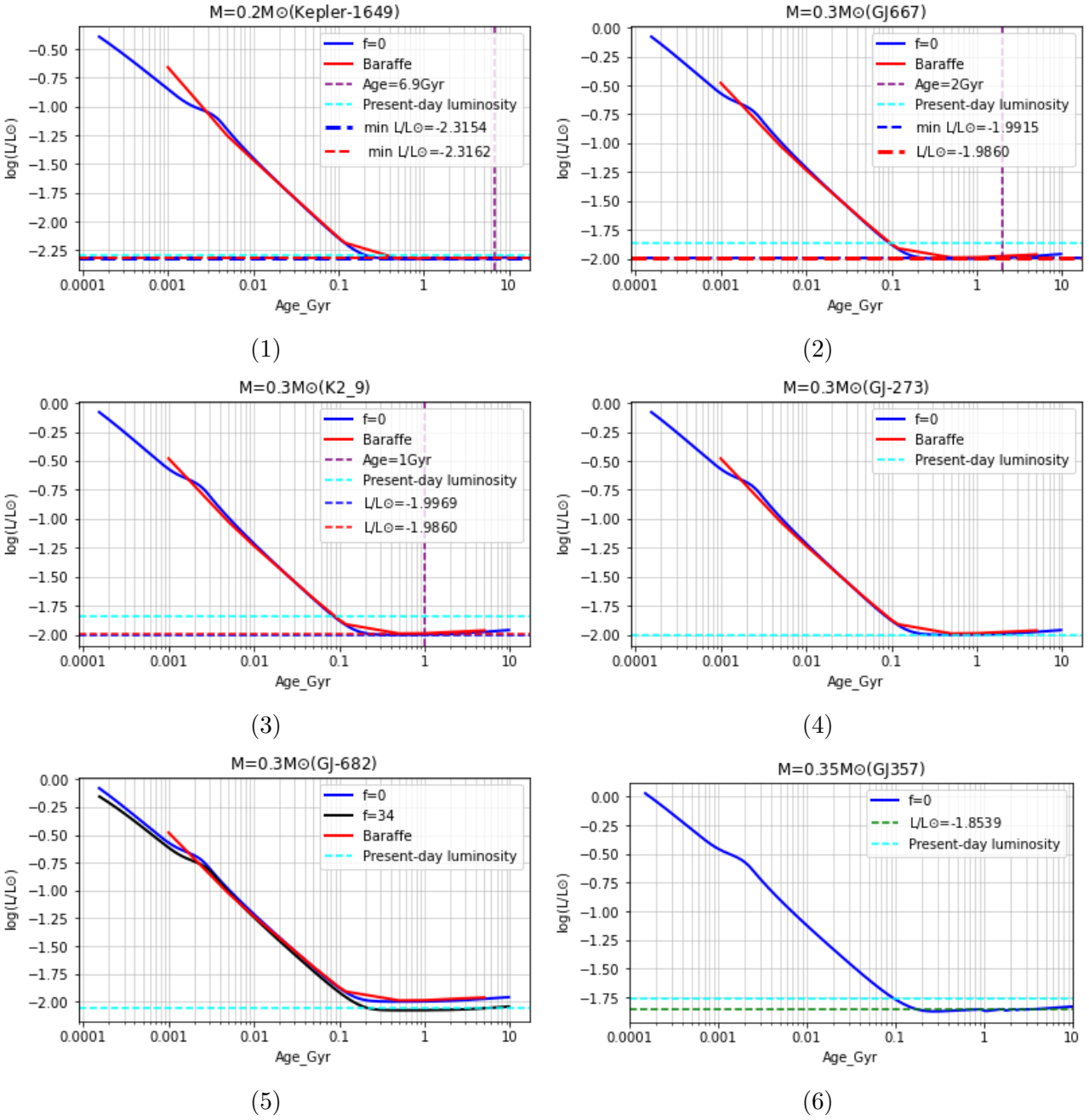

Figure 5.4: Evolution of Luminosity and preset-day bolometric luminosity for stars with masses from $0.02M_{\odot}$ to $0.35M_{\odot}$, considering two different evolutionary models (Baraffe et al., 2015; Somers et al., 2020).For model of Somers et al. (2020)we considered spot fraction of 0 and 34% for GJ-686 to show the differences between them, but for the other stars we only assumed spot fraction equal to zero.

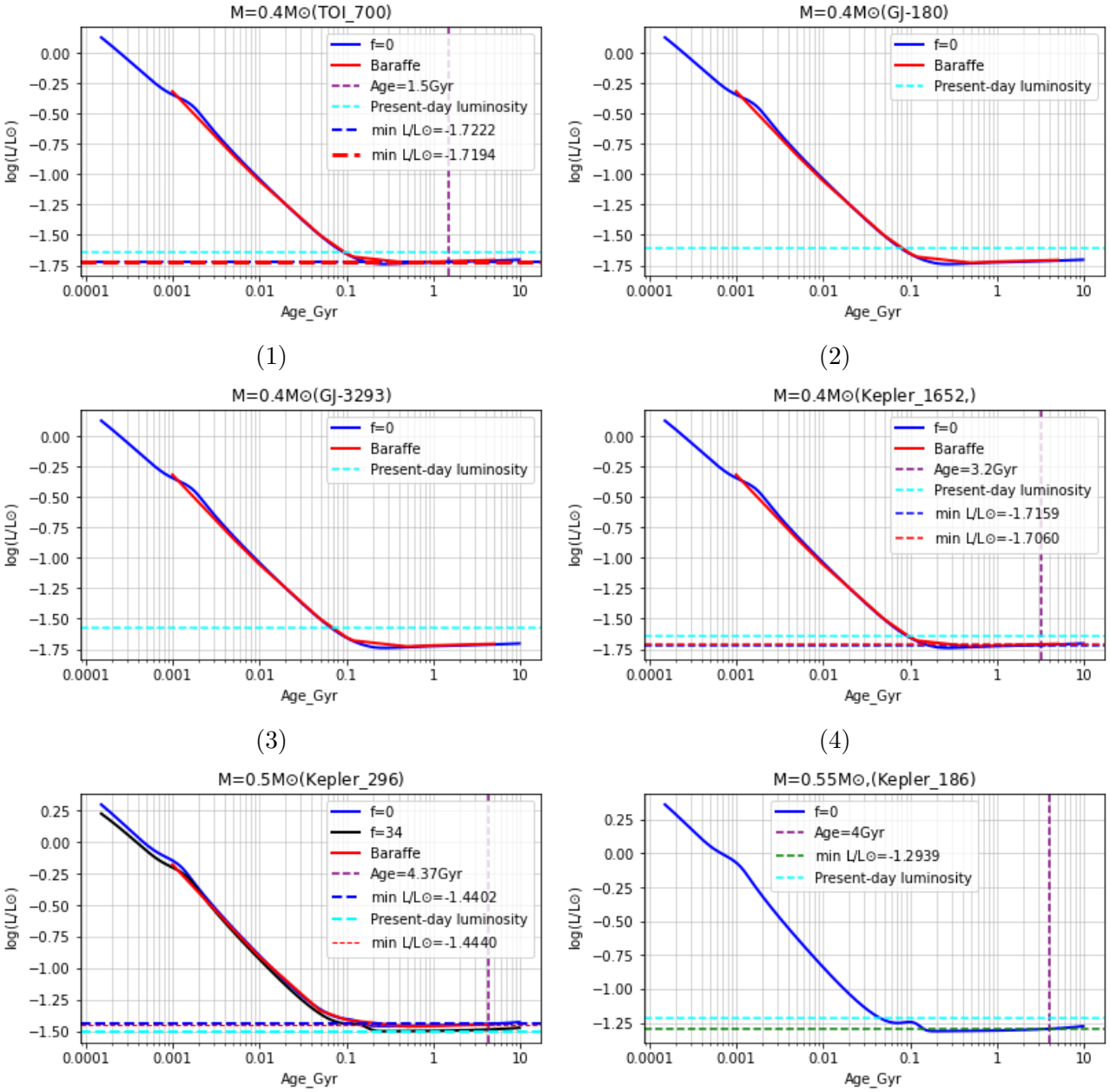

,

Figure 5.5: Evolution of Luminosity and preset-day bolometric luminosity for stars with masses from $0.4M_{\odot}$ to $0.55M_{\odot}$, considering two different evolutionary models (Baraffe et al., 2015; Somers et al., 2020).For model of Somers et al. (2020) we considered spot fraction of 0 and 34% for Kepler-296 to show the differences between them, but for the other stars we only assumed spot fraction equal to zero.

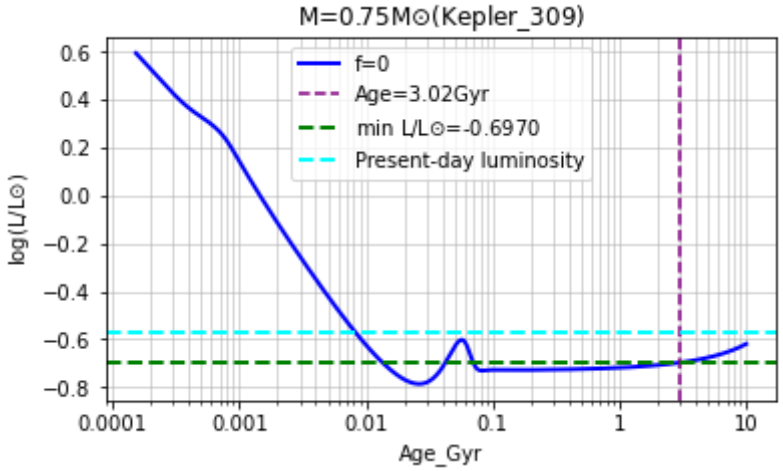

Figure 5.6: Evolution of Luminosity and preset-day bolometric luminosity for star with mass of $0.75M_{\odot}$, considering evolutionary model of (Somers et al., 2020).We considered only the spot fraction equal to zero.

Considering the age of planets (assumed to be the same as their host stars) and the associated evolutionary model, we plot the minimum required luminosity for each planet's host star to maintain the planet within the habitable zone. As it is observed the minimum luminosity of both models appears to be quite similar. However, there are some exceptions in these plots.

Figs. 5.3(1), 5.3(2), 5.3(3), 5.3(5) and 5.3(6) show the evolution of luminosity for stars with $M=0.08M_{\odot}$ like as TRAPPIST-1, $M=0.09M_{\odot}$ like as Teegardens' Star, $M=0.011M_{\odot}$ like as Proxima and GJ 1002, $M=0.17M_{\odot}$ like as TIO-1227 and Wolf 1069 from the models of Baraffe et al. (2015) because there was not any similar masses in the model of Somers et al. (2020). However, as it is observable we simulate evolution of luminosity for $M=0.15M_{\odot}$ like as LHS-1140 from both models of evolutionary.

We observe a significant luminosity discrepancy in Fig. 5.3(5).

Fig. 5.3(5): This plot illustrates star TIO-1227 with a mass of $M=0.17M_{\odot}$. It is observed that its present-day luminosity (`https://exoplanetarchive.ipac.caltech.edu/overview/TOI-1227#star_TOI-1227_collapsible`)is lower than the luminosity required for a star of this mass range to be in the habitable zone. Regarding our calculation from models of Baraffe et al. (2015) log $LL_{\odot}$ for TIO-1227 is -1.554 but from the data we have, it is equal to -1.81. Of course we obtained this amount considering the age of TIO-1227 equal to 0.011Gyr (Mann et al., 2022). We conclude that either the planet TIO-1227 b is not in the habitable zone, or the Baraffe evolutionary model encounters challenges in this mass range, or there may be inaccuracies in the data for this star.

Fig. 5.3(6): This figure shows star Wolf 1069 with mass of $M=0.167M_{\odot}$ as it was the closest mass in the model we utilized. Once again, it is observed that the present-day luminosity is less than the minimum required luminosity for a planet in its orbit to be in the habitable zone, similar to the observation in Fig. 5.3(5). However, the differences in luminosities in this plot are not substantial. It is conceivable that considering some fraction of spots on the star could yield the desired result, but it's worth noting that in the Baraffe model, we don't have the option to account for different spot fractions to investigate this problem.

In Figs. 5.4(1) to (5), we drew the evolution of luminosity from both models. but for Fig. 5.4(6) we only plotted for the model of Somers et al. (2020) as there was not the same rage of mass in the model of Baraffe et al. (2015).

Figs. 5.4(5): We observe that for GJ-682 with a mass of M=0.27 $M_{\odot}$, the evolutionary model supports them when considering a spot fraction equal to or more than 34 percent.

In Figs. 5.5(1) to (5), we drew the evolution of luminosity from both models. but for Fig. 5.5(6) again we only plotted for the model of Somers et al. (2020) as there was not the same rage of mass in the model of Baraffe et al. (2015).

Fig. 5.5, representing Kepler-296 with a mass of M=0.5M⊙, illustrates that, by considering the present-day luminosity of Kepler-296 (log (L/L⊙)=-1.56), the models of Somers et al. (2020) with f=0 and Baraffe et al. (2015) suggest that this star's luminosity is insufficient for the habitable zone. However, according to the model of Somers et al. (2020), if a spot fraction equal to or greater than 34% is considered, its luminosity falls within the range required for the habitable zone.

Fig. 5.6 depicts the luminosity evolution for stars with M=0.75 $M_{\odot}$, such as Kepler-309, based on the evolutionary model by Somers et al. (2020). It is noticeable that the trend of luminosity changes for this mass of stars differs from those presented in the previous plots. However, in this study, we will not delve into discussing these alterations.

5.4 Inner Edge of the HZ (IHZ)

Recently, several low mass planets are discovered around M stars, so calculating of these stars' habitable zone is becoming significantly important(Kopparapu et al., 2013). Kopparapu et al. (2016) estimated the habitable zones (HZs) around stars by considering the variety range of stellar effective temperatures(2600−7200K), particularly for M dwarfs. In fact, they used the HZ around the Sun as the base of their estimation. The solar fluxes (S_{eff}), reach a minimum near the Outer Habitable Zone (OHZ). This occurs because the atmosphere becomes optically dense across all infrared wavelengths, Also, planetary reflective increases due to Rayleigh scattering caused by CO_2 condensation. Kopparapu et al. (2016) computed the value of S_{eff} using their climate model which varies based on the type of star being considered.

$$S_{\text{eff}} = S_{\text{eff}_{\odot}} + aT_{\star} + bT_{\star}^2 + cT_{\star}^3 + dT_{\star}^4 \tag{5.1}$$

where $T_{\star} = T_{\text{eff}} - 5780$ K and the coefficients are listed in Table 3 for various habitability limits. [19] The corresponding HZ distances can be calculated using the relation

$$d = \left(\frac{L/L_{\odot}}{S_{\text{eff}}}\right)^{0.5} \text{AU} \tag{5.2}$$

where $L/L_{\odot}$ is the luminosity of the star compared to the Sun.

Constant	Runaway Greenhouse	Maximum Greenhouse
$S_{eff\odot}$	1.107	0.356
a	1.332e−4	6.171e−5
b	1.580e−8	1.698e−9
c	-8.308e−12	-1.931e−15
d	-3.198e−12	-5.575e−16

Table 5.2: Coefficients to calculate stellar Flux in Equation5.1, associated with HZ, for stars' temprature in range of 2600-7200 K (Kopparapu et al., 2013)

We used these equations to determine the Inner boundary of the Habitable Zone (IHZ) for our target planets' host stars (considering their mass)form evolutionary model of Baraffe et al. (2015) and Somers et al. (2020). We did it for two different phases, Runaway Greenhouse and Maximum Greenhouse, moreover for two different constants fluxes, $0.9S_{\oplus}$ (non-synchronous planet)and $01.5S_{\oplus}$(synchronous planet) asRibas et al. (2016) considered. also we showed the present-day inner distance of different planets of star(which are exist in our target list(Table5.1)assuming no migration and that they originally formed at these distances.

We investigated the evolution of the HZ inner edge for nineteen stars (with considering their mass) in nineteen plots(Figs. 7, 8 and 9). In the presented plots, different line colors and styles represent distinct models and scenarios which are common in all plots:

Green Lines, Baraffe et al. (2015) Model: These lines correspond to the Baraffe model, with variations denoted by different stellar irradiance (S_p) values.

Red Lines, Somers et al. (2020) Model, f=0: The red lines depict the Somers model with a fixed flux (f=0), considering different stellar irradiance values.

Black Lines, Somers et al. (2020),f=85: This line represents the Somers model with a fixed flux (f=85) for various stellar irradiance values.

Horizontal lines: These lines represent the present-day distances of planets from their host stars

vertical lines: These lines show the age of stars or the minimum ages that planets could have to be in Habitable zone.

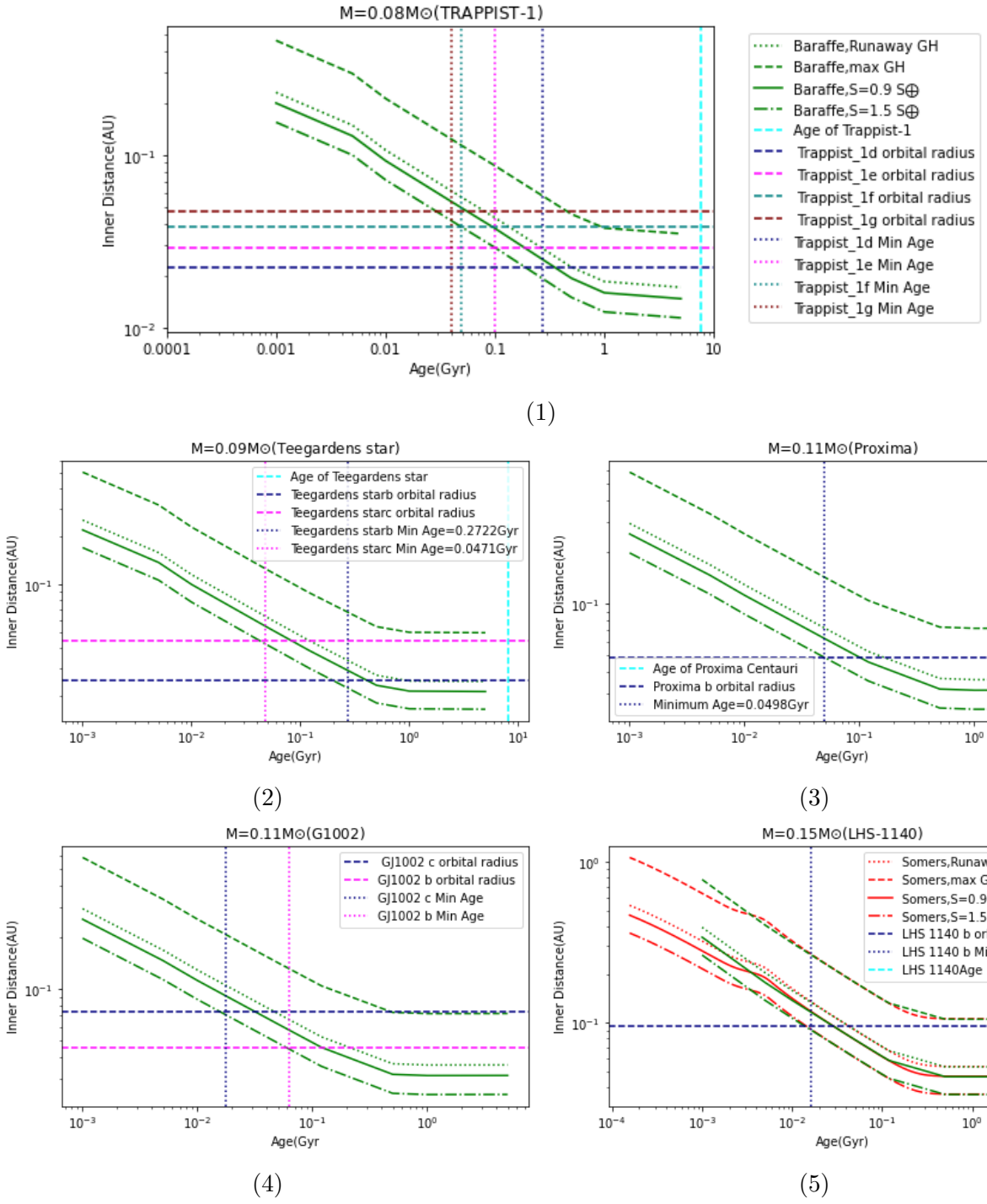

Figure 7: Comparing the evolution of HZ inner distance for different stars mass(M=0.08$M_\odot$ to M=0.15$M_\odot$ and their planets, considering two evolutionary models of Somers et al. (2020); Baraffe et al. (2015)

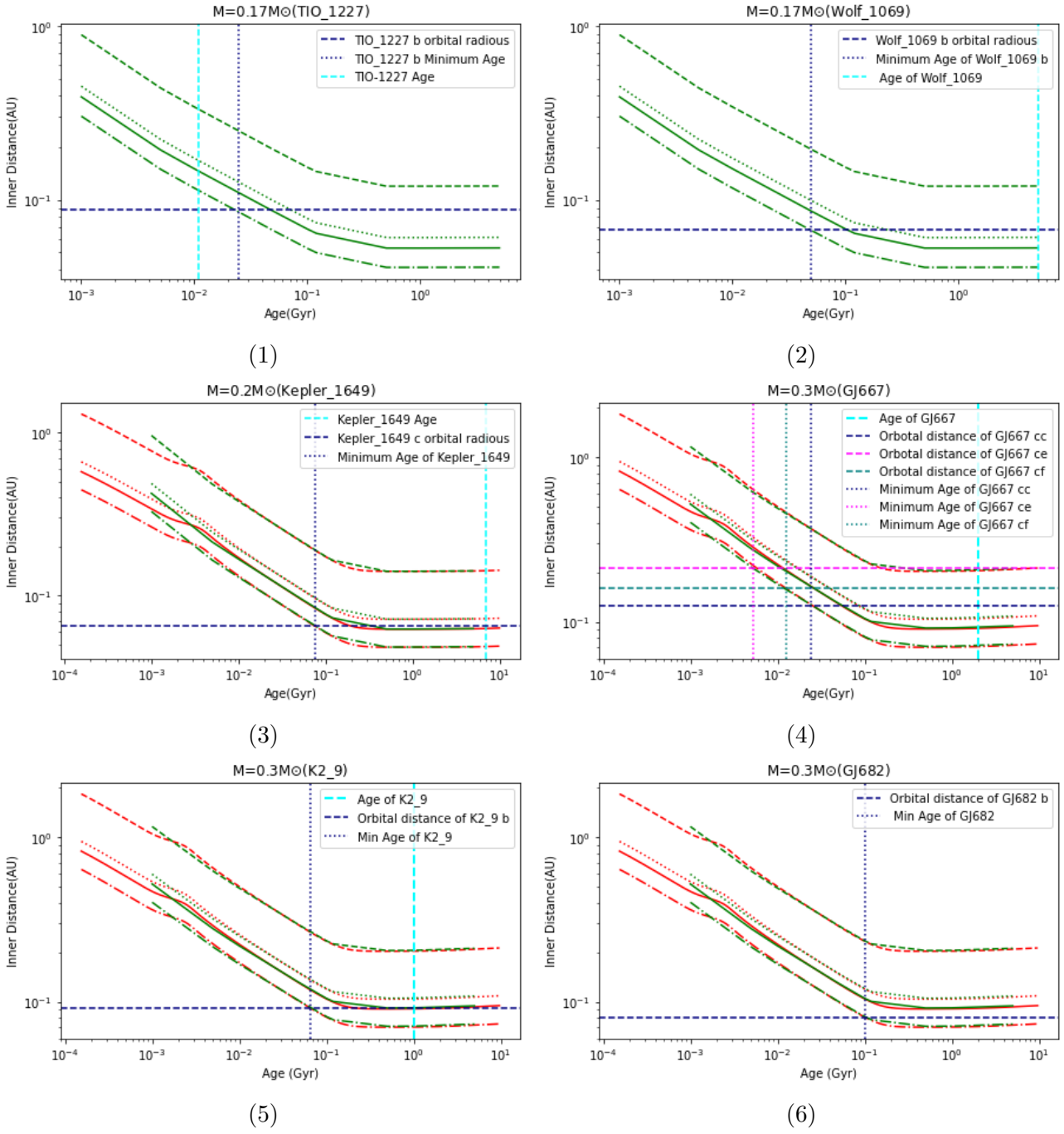

Figure 8: Comparing the evolution of HZ inner distance for different stars mass(M=0.17$M_\odot$ to M=0.3$M_\odot$ and their planets, considering two evolutionary models of Somers et al. (2020); Baraffe et al. (2015)

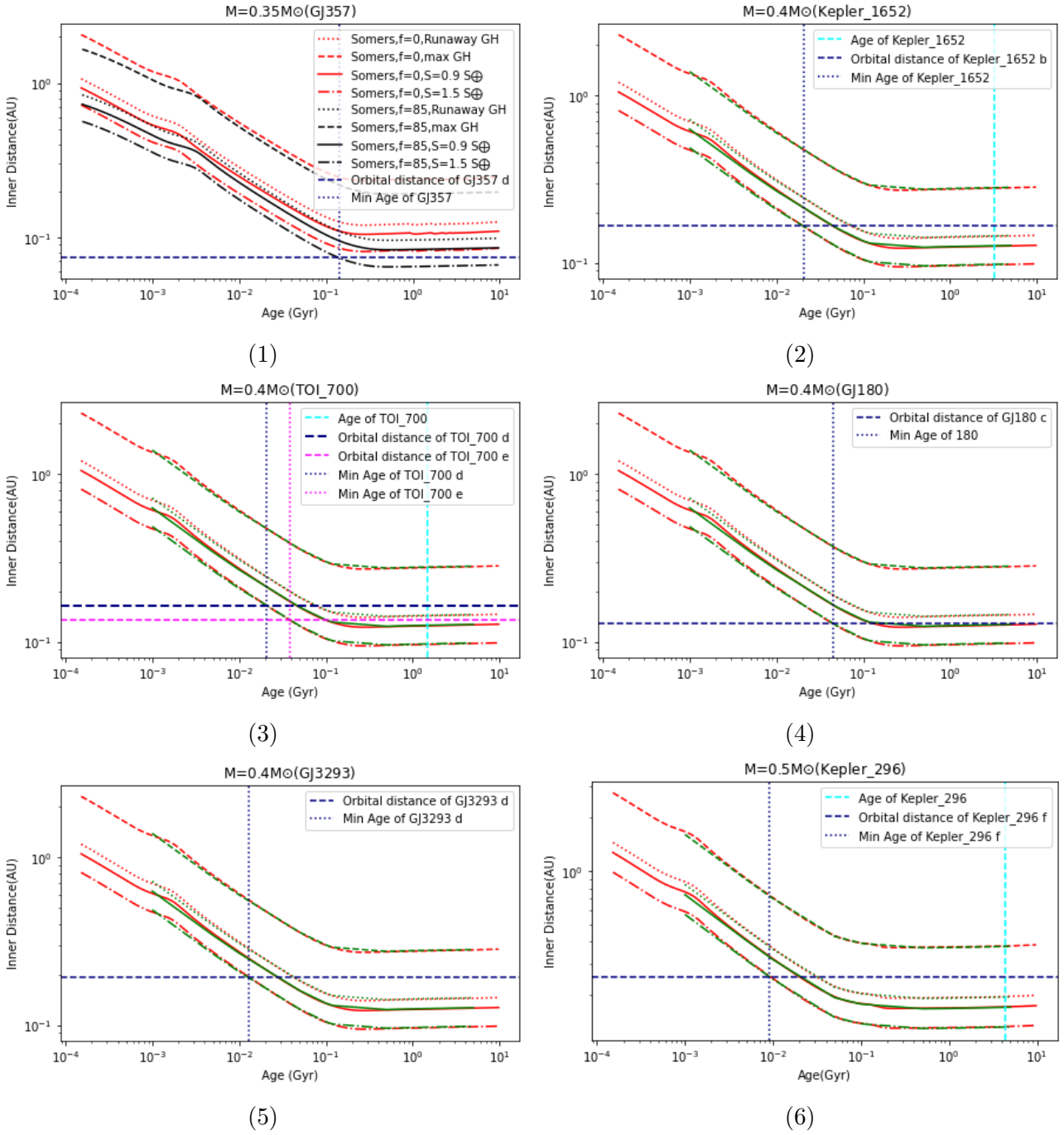

Figure 9: Comparing the evolution of HZ inner distance for different stars mass(M=0.35$M_\odot$ to M=0.5$M_\odot$ and their planets, considering two evolutionary models of Somers et al. (2020); Baraffe et al. (2015)

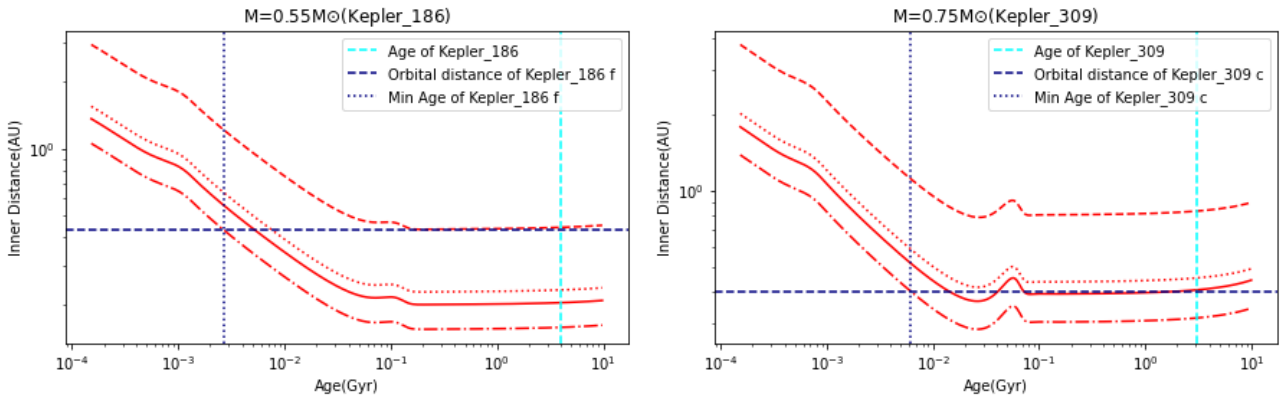

(1) (2)

Figure 10: Comparing the evolution of HZ inner distance for different stars mass(M=0.55$M_\odot$ and M=0.75$M_\odot$ and their planets, considering evolutionary model of Somers et al. (2020)

Fig.7(1): model of Somers et al. (2020) does not support the mass equal to $0.08M_\odot$. Therefore, for TRAPPIST-1, we only considered the model by Baraffe et al. (2015) and plotted the present-day distances of the four outer planets of it, which are considered HZ exoplanets. As observed, TRAPPIST-1d and TRAPPIST-1e are not supported in evolutionary model of the maximum GH phase (obtained using Equations 5.1 and 5.2 and coefficients from Table5.2), but the other two outer planets are supported by all four phases.

Fig.7(2): Mass= $0.9M_\odot$ is also only supports by Baraffe et al. (2015). For Teegarden's star c and b we plot the present-day orbital distance. As we observe maximum GH phase does not support them. But Runaway phase and constant fluxes cover them.

Fig. 7(3): The mass of Proxima Centauri is approximately $0.12M_\odot$, but neither Somers et al. (2020) nor Baraffe et al. (2015) supported this mass. We considered the closest mass to it, $M = 0.11M_\odot$. It is observed that only the maximum GH phase does not cover it.

Fig.7(4): It is shown the orbital distances of G1002 b and c. As it is observed, the G1002 c is covered by all different assumtions, however, maximum GH phase does not cover the GJ1002b. Ofcourse, we do not have any information about the age of G1002 and due to those planets considered as HZ planets, the age of star should be higher than the 0.226 Gyr (regarding the numerical data we obtained frm our plots)to be supported by these plots.

Fig.7(5): M=$M = 0.15M_\odot$ is supported by both evolutionary models that we used.(Somers et al., 2020; Baraffe et al., 2015). It is observed that only maximum GH phase does not cover it.

Fig.8(1): In this plot, the horizontal line represents the present-day orbital distance of TIO-1227 b (0.0886 AU)and light blue vertical line represents the age of TIO-1227 equal to 0.011Gyr (Mann et al., 2022), which we considered it as the age of TIO-1227 b; and dark blue vertical line shows the minimum age that TIO-1227 needs to have for being in habitable zone regarding its distance from the host star and Evolutionary models of Baraffe et al. (2015).This plot is one of the exceptions we encountered in our study. According to the age of this planet (0.011 Gyr), it must be in a distance of 0.117 AU (according to our calculation) to be considered as a HZ planet but the data show that its inner distance is 0.0886 AU. If the data regarding the distance are correct, the age of planet must be 0.024 Gyr instead of 0.011 to placed this planet in HZ. It seems that the data we have are not enough for investigating this star's IHZ.

Fig.8(2): The mass of Wolf-1069 is equal to 0.167 $M_\odot$. From the models that we considered M=$0.17M_\odot$ wast the closest mass to it. As it is observed only the maximum GH phase does not

support it.

Fig.8(3): We found out the mass equal to the mass of Kepler-1649 (M=0.2$M_\odot$) in both evolutionary modelsSomers et al. (2020); Baraffe et al. (2015). Both models show almost the same trends. it is illustrated non of two phase of Runaway GH and maximum GH cover this planet's data. only the evolutionary models which we considered the constant flux ($S_p = 0.9S_\oplus$ and $S_p = 1.5S_\oplus$) in them work as well.

Fig.8(4): This plot shows both evolutionary models Somers et al. (2020); Baraffe et al. (2015) for GJ667. Its mass is equal to 0.33$M_\odot$ and we considered it as M=0.3$M_\odot$. We observe that both models with three different S_p($S_p = 0.9S_\oplus$ and $S_p = 1.5S_\oplus$ and S_p = Runaway GH phase) sopurt it.

Fig.8(5): This plot illustrates evolutionary model for K2-9. We observe that only models which considered constant S_p support this star's data.

Fig.8(6): As it is observable in this plot, which shows the evolution of GJ682, only models considered $S_p = 1.5S_\oplus$ is covered this star's data. As this constant S_p is considered for tidal locked planets (Ribas et al., 2016), it may conclude that GJ682 b is a tidal locked planet. However to reach such conclusion we need much more data and calculation that are not included in this study.

Fig.9(1): GJ357, with a mass of 0.35$M_\odot$, is another exception we encountered in our study. Although it is not the only one that is supported just by models considering Sp=1.5S$\oplus$, this exception is attributed to the fraction of spots used for this plot. "However, we do not know the real age of GJ357. Considering GJ357 b's orbital distance, the only evolutionary model that covers this star and planet's data is the one with a spot fraction equal to 85%. Moreover, it could conclude that this planet is tidal locked as the the planet in Fig.8(6).

Fig.9(2): This plot shows Kepler-1652 with M=0.4$M_\odot$. It is observed that only models considered for maximum GH does not support it.

Fig.9(3): The mass of TIO-700 is equal to 0.416 M$M_\odot$ that the closest mass in two models that we considered here is M=0.4$M_\odot$. It is obvious that models with considering constant fluxes support this star's data, but, the models with considering Runaway GH phase only support the planet TIO-700 d.

Fig.9(4): Mass of GJ180 is equal to 0.43 that we considered it as M=0.4$M_\odot$. We can observe that non of two phase of Runaway GH and maximum GH support it. We do not know the age of GJ180, considering GJ180c as a habitable exoplanet, its age should be higher than 0.272 Gyr to fit those models.

Fig.9(5): Mass of GJ3293 is equal to 0.42$M_\odot$ and closest mass to it from the models Somers et al. (2020); Baraffe et al. (2015), was M=0.4$M_\odot$. This plot illustrates that the only phase does not support it is the maximum GH phase. The age of this star is not known yet. From the orbital distance of GJ3293 d and considering that it is in HZ and also covered by all three assumptions of different fluxes($S_p = 0.9S_\oplus$, $S_p = 1.5S_\oplus$, S_p = Runaway GH phase), its age should be at least 0.0423Gyr.

Fig.9(6): This plot exhibits evolutionary models of Kepler-296 which has mass equal to 0.5$M_\odot$. It is supported by three different fluxes ($S_p = 0.9S_\oplus$, $S_p = 1.5S_\oplus$, S_p = Runaway GH phase).

Fig.10(1): We considered mass of Kepler-186 equal to 0.55$M_\odot$ as it was closest mass in evolutionary model of Somers et al. (2020)(The real mass of Kepler-186 is 0.54 and we could not file similar mass for it in Baraffe et al. (2015) model). It reveals the model with all four different fluxes support the data.

Fig.10(2): Evolutionary model of Kepler-309 with M=0.75$M_\odot$ is demonstrated in this plot. We can observe that evolutionary model of Somers et al. (2020) support it only when consider constant fluxes.

5.5 Time duration before entering HZ and loss of water

Having the stars' evolutionary trend, we can find out the time each planet enter the HZ. This comparative approach allows for the determination of the time elapsed since the planets in these systems transitioned into or out of the habitable zone. The age of the planets was considered to be equivalent to the age of their host stars. Consequently, this analysis sheds light on the duration during which the planets were not within the habitable zone, the period that there is the possibility of causing the evaporation of water because of intense irradiation which providing crucial information for understanding the potential habitability timeline of these planetary systems. We calculated this time interval for all of our target planets considering four different assumptions(Table5.3. As it is mentioned before, for a synchronized planet we considered S_p= 1.5 due to the presence of clouds at the substellar point enables the planet to orbit much closer(S_p=1.5$S_\oplus$) (Yang et al., 2013; Kopparapu et al., 2016) and for non-synchronous planet we assumed S_p= 0.9 $S_\oplus$as Ribas et al. (2016) did. Moreover, we calculate this time considering Runaway phase Greenhouse and Maximum Greenhouse where we taking into account that planets' received flux (S_p) changes due to the effective temperature rather than assuming it constant (Equation 5.1)(Kopparapu et al., 2013).

TIO-1227 b*: As we mentioned before (Fig.8(1)), the age that is reported for this planet (Mann et al., 2022)and the orbital distance that it has, does not show that this planet is in habitable zone, but here, we considered TIO-1227 b is a habitable exoplanet, and found out the minimum ages that it could be out of HZ (before entering to HZ). As mentioned in chapter 3, Bolmont et al. (2017) and Ribas et al. (2016) approximated the water mass loss for planets of Trappist-1 and Proxima Centauri b. In this study, we considered their estimations and compared them with our obtained results to determine whether these target planets are capable of retaining water or not. As we calculated the time of each planet before entering HZ, we can investigate the amount of water loss considering equation bellow:

$$m = \epsilon \frac{\pi R_{\rm p}^3}{\mathcal{G} M_{\rm p}} \int_0^t \frac{F_{\rm XUV}}{(a/1{\rm au})^2}\ {\rm d}t \tag{5.3}$$

According to Bolmont et al. (2017), planets orbiting more massive stars experience a higher degree of water loss. Moreover, planets with higher mass experience the higher rate of water mass loss than the lower mass planets. Now we are able to compare our obtained results with the previous works to make a conclusion.

Due to lack of information about our target planets' atmosphere and amount of fluxes they receive, we only compare those with masses close to that of Trappist-1 and Proxima Centauri to draw conclusions about their water content.

From the table5.1, GJ103903(Teegarden's star) has comparable mass and spectral type to Trappist-1. Also, the orbital period of Teegarden's star b and c are similar to the orbital distance of Trappist-1 d and g, respectively. Regarding (Bolmont et al., 2017) Trappist-1 d lost about $3EO_H$ before entering the habitable zone. Comparing this with Teegarden's star b, we observe from Table5.3 that Teegarden's star b spent about twice as much time in the Runaway phase. Consequently, we can conclude that it has lost more mass than Trappist-1 d. Also, the mass of Teegarden's star b is higher than the mass of Trappist-1 d which increases the mass loss rate of Tgarden's star b. Comparing Trappist-1 g and Teegarden's c, despite of their simillar masses, Teegarden's c spent about 1.5 time more time prior entering HZ than the Trappist-1 g which will cause to loss more mass.

Planet	S_p= 1.5 $S_\oplus$	S_p= 0.9 $S_\oplus$	Runaway GH	Maximum GH
Trappist-1 d	0.183	0.361	0.444	
Trappist-1 e	0.099	0.189	0.295	
Trappist-1 f	0.049	0.096	0.156	0.952
Trappist-1 g	0.026	0.051	0.0789	0.462
Teegardens star b	0.214	0.410	0.966	
Teegardens star c	0.046	0.086	0.117	
Prox Cen B	0.0497	0.101	0.181	
G1002 b	0.0620	0.119	0.226	
G1002 c	0.0235	0.0408	0.045	
LHS-1140 b	0.0197	0.030	0.039	
TIO-1227 b*	0.025	0.0425	0.075	
Wolf-1069 b	0.050	0.105	0.225	
Kepler-1649 c	0.076	0.201		
GJ 667 Cc	0.036	0.050	0.083	
GJ 667 Ce	0.005	0.013	0.025	
GJ 667 Cf	0.018	0.029	0.040	
K2-9 b	0.066	0.162		
GJ 682 b	0.102			
GJ 357 d	0.141			
Kepler-1652 b	0.021	0.044	0.072	
TOI-700 d	0.021	0.049	0.0826	
TOI-700 e	0.039	0.100		
GJ 180 c	0.044	0.127		
GJ 3293 d	0.0128	0.027	0.042	
Kepler-296 f	0.009	0.200	0.030	
Kepler-186 f	0.003	0.005	0.008	0.186
Kepler-309 c	0.006	2.93		

Table 5.3: Time Intervals(Gyr) Outside the Habitable Zone for our Target Planets Considering Different S_{eff}

Furthermore, we can comparing Proxima Centauri b with GJ1002 b,c and LHS-1140 b due to their host stars' mass are close to each other. (Ribas et al., 2016) calculated less than $1EO_H$ loss for Proxima b in its initial Runaway phase and considered the most stringent conditions for background atmosphere during Runaway phase, they explained that Proxima b might have experienced water lost of 16–21 EO_H during its age. On the other hand, they suggested that it is possible that Proxima b retained its background atmosphere over the 4.8 billion years of evolution,which means it may have lost the lower amount of water and concluded that Proxima b could have liquid water on its surface today and could be considered as a promising candidate for a habitable planet.

From Table5.1, Proxima Centauri and GJ1002 have the same mass and spectral type. Additionally, Proxima b and GJ1002 b exhibit nearly identical orbital periods, orbital distances, and also they have similar $M_p$sini values (0.00340 M_{Jup}). the only difference between them is the time

they spent in Runaway phase where GJ1002 b spent about 25% more time which may constrain its habitability; however, we do not have any information about GJ1002's age, so considering the conclusion of Ribas et al. (2016), if the age of GJ1002 is similar or more than Proxima's, there's a possibility of liquid water on its surface. Furthermore, GJ1002 c has a greater orbital distance than Proxima b, but with slightly higher $M_p$sini (0.00428 M_{Jup}), but the difference is not substantial if considering its significantly less time in the Runaway phase before entering the habitable zone which could be concluded of higher water content.

Comparing Proxima b with LHS-1140 b from table5.1, they have almost the same host star mass, age and spectral type, while the orbital radius of LHS-1140 b is about twice that of Proxima b. From the table5.3, we observe the time Proxima b spent before entering the HZ is about four times more than the time LHS-1140 b spent.Consequently, we might infer that LHS-1140 b has more water content than Proxima b. On the other hand, the mass of LHS-1140 is about five times greater than the mass of Proxima b, and as mentioned before, a higher mass of the planet will result in a higher rate of water mass loss. Therefore, to draw a solid conclusion we need more details such as the amount of different types of flux that planets receive, exoplanets' atmosphere, temperature and climate modeling.

Chapter 6

Summary

Regarding the intricate details of the irradiation environment surrounding planets in the habitable zone (HZ), we focused our attention on M-type stars. The selection of M-type stars is motivated by their unique characteristics, which we explored in detail to justify our choice.

Given the importance of the irradiation environment, we categorized the various types of irradiation that planets may encounter. Recognizing the fundamental importance of water for the possibility of life, we investigated methods to estimate its presence or absence on these distant celestial bodies.

Two significant M-type stars, Proxima Centauri and TRAPPIST-1, became the subjects of our study, as we wanted to consider previous research on the planets within these systems as benchmarks to compare and contrast our findings.

Expanding our scope, we introduced additional criteria beyond M-type stars. Planets with a mass less than 10 Earth masses, a continuous habitable zone existence throughout their lifespan, and an age less than 10 Gyrs were considered.

A crucial aspect of our exploration involved tracking the evolution of luminosity for selected stars (nineteen stars) and the corresponding changes in their habitable zone's inner edge over time. This temporal analysis allowed us to determine the duration planets may spend outside the habitable zone due to stellar evolution.

Upon careful analysis of the plotted data, certain trends come to light:

The analysis of Luminosity-Age plots indicates a discrepancy between the available information for TIO-1227 ($\log(L_*/L_\odot)$=-1.81) and the evolutionary model proposed by Baraffe et al. (2015)($\log(L_*/L_\odot)$=-1.55). Additionally, it is noteworthy that the data for GJ-682 and Kepler-296 aligns with the model only when considering a spot fraction equal to or greater than 34%.

The simulations of Inner Distance-Age relationships reveal that, among our target planets (Table 5.1), only TRAPPIST-1 f and g, GJ1002 c, GJ667 ce, and Kepler-186 f have entered the maximum Greenhouse (GH) phase. Surprisingly, the data for TIO-1227 indicates that this planet still lies outside the habitable zone (distance of planet must be 0.117 instead of 0.088 or the age of planet must be 0.024 Gyr instead of 0.011 Gyr to place in HZ). Furthermore, we observe that GJ-357 d could be situated in the habitable zone only if we consider a spot fraction of its host star equal to 85%.

As we lacked data on the atmospheres and received fluxes of our target planets, we compared Teegardens' star b and c with TRAPPIST-1 d and g. Similarly, we compared GJ1002 b and c with LHS-1140 b and Proxima b because their host stars have similar masses and spectral type as in Table6.1 .

Star	$M_*/M_\odot$	Sp-type	Planet	M_p (M_{Jup})	$M_p \sin i$ (M_{Jup})	a (AU)	Time (Gyr)
TRAPPIST-1	0.08	M8	d	0.0013		0.02227	0.444
TRAPPIST-1	0.08	M8	g	0.0422		0.04683	0.0789
GJ10393 [a]	0.09	M7.0 V	b		0.00330	0.0033	0.966
GJ10393	0.09	M7.0 V	c		0.00349	0.0443	0.117
Proxima	0.12	M5.5 V	b		0.00337	0.0485	0.181
GJ 1002	0.120	M5.5 V	b		0.00340	0.0457	0.226
GJ 1002	0.120	M5.5 V	c		0.00428	0.0738	0.045
LHS 1140	0.146	M4.5 V	b		0.0192	0.0957	0.39

Table 6.1: Information of Planets with their main characteristics. a(AU) is the semi axis of planet. Time(Gyr) is the time duration than planet spent before entering HZ, here we considered the Runaway GH phase time duration which we calculated

[a] GJ103903 is the other name of Teegardens' star

From this comparison, we conclude that Teegardens' star b and c will lose a higher water mass than TRAPPIST-1 d (according to Bolmont et al. (2017), TRAPPIST-1d lost its water less than 3EO).

Comparing to Proxima b, there is a possibility for GJ1002 b to have liquid water on its surface, and there is also a possibility that GJ1002 c has even higher water content than Proxima b (ragarding Ribas et al. (2016), Proxima b lost its water mass about 16 to 21 EO). Regarding LHS-1140b, we cannot draw a clear conclusion as it spent 4.64 times less time outside the habitable zone, on the other hand, has about 5 times greater mass than Proxima b.

Surely, understanding the evolutionary pattern of the XUV emission from the star, atmosphere and climate models are crucial for estimating the potential mass loss of water during the runaway phase of the planet. A detailed exploration of these aspects can be covered by future research endeavors.

Bibliography

Abrevaya, X. (2013). Astrobiology in argentina and the study of stellar radiation on life. *Boletin de la Asociacion Argentina de Astronomia La Plata Argentina*, 56:113–122.

Anglada-Escudé, G., Amado, P. J., Barnes, J., Berdiñas, Z. M., Butler, R. P., Coleman, G. A., de La Cueva, I., Dreizler, S., Endl, M., Giesers, B., et al. (2016). A terrestrial planet candidate in a temperate orbit around proxima centauri. *Nature*, 536(7617):437–440.

Baraffe, I., Chabrier, G., Allard, F., and Hauschildt, P. (1998). Evolutionary models for solar metallicity low-mass stars: mass-magnitude relationships and color-magnitude diagrams. *arXiv preprint astro-ph/9805009*.

Baraffe, I., Homeier, D., Allard, F., and Chabrier, G. (2015). New evolutionary models for pre-main sequence and main sequence low-mass stars down to the hydrogen-burning limit. *Astronomy & Astrophysics*, 577:A42.

Battistuzzi, M., Cocola, L., Claudi, R., Pozzer, A. C., Segalla, A., Simionato, D., Morosinotto, T., Poletto, L., and La Rocca, N. (2023). Oxygenic photosynthetic responses of cyanobacteria exposed under an m-dwarf starlight simulator: Implications for exoplanet's habitability. *Frontiers in Plant Science*, 14:1070359.

Belu, A. R., Selsis, F., Raymond, S. N., Pallé, E., Street, R., Sahu, D., Von Braun, K., Bolmont, E., Figueira, P., Anupama, G., et al. (2013). Habitable planets eclipsing brown dwarfs: strategies for detection and characterization. *The Astrophysical Journal*, 768(2):125.

Bialy, S., Sternberg, A., and Loeb, A. (2015). Water formation during the epoch of first metal enrichment. *The Astrophysical Journal Letters*, 804(2):L29.

Birky, J., Barnes, R., and Fleming, D. P. (2021). Improved constraints for the xuv luminosity evolution of trappist-1. *Research Notes of the AAS*, 5(5):122.

Bolmont, E., Raymond, S. N., Leconte, J., and Matt, S. P. (2012). Effect of the stellar spin history on the tidal evolution of close-in planets. *arXiv preprint arXiv:1207.2127*.

Bolmont, E., Selsis, F., Owen, J. E., Ribas, I., Raymond, S. N., Leconte, J., and Gillon, M. (2017). Water loss from terrestrial planets orbiting ultracool dwarfs: implications for the planets of trappist-1. *Monthly Notices of the Royal Astronomical Society*, 464(3):3728–3741.

Boss, A. P. (1997). Giant planet formation by gravitational instability. *Science*, 276(5320):1836–1839.

Brugger, B., Mousis, O., Deleuil, M., and Lunine, J. (2016). Possible internal structures and compositions of proxima centauri b. *The Astrophysical Journal Letters*, 831(2):L16.

Charbonneau, D., Brown, T. M., Latham, D. W., and Mayor, M. (1999). Detection of planetary transits across a sun-like star. *The Astrophysical Journal*, 529(1):L45.

Claudi, R., Erculiani, M., Galletta, G., Billi, D., Pace, E., Schierano, D., Giro, E., and D'Alessandro, M. (2016). Simulating super earth atmospheres in the laboratory. *International Journal of Astrobiology*, 15(1):35–44.

Cromie, G. A., Connelly, J. C., and Leach, D. R. (2001). Recombination at double-strand breaks and dna ends: conserved mechanisms from phage to humans. *Molecular cell*, 8(6):1163–1174.

Dartnell, L. R. (2011). Ionizing radiation and life. *Astrobiology*, 11(6):551–582.

Diffey, B. (1991). Solar ultraviolet radiation effects on biological systems. *Physics in medicine & biology*, 36(3):299.

Dominguez, G. (2016). On the abundance of water in extrasolar planetary systems as a function of stellar metallicity. In *American Astronomical Society Meeting Abstracts# 228*, volume 228, pages 404–02.

Ehrenreich, D., Hébrard, G., Des Etangs, A. L., Sing, D. K., Désert, J.-M., Bouchy, F., Ferlet, R., and Vidal-Madjar, A. (2007). A spitzer search for water in the transiting exoplanet hd 189733b. *The Astrophysical Journal*, 668(2):L179.

Encrenaz, T. and Mizon, B. (2007). *Searching for Water in the Universe*. Springer.

Fleming, D. P., Barnes, R., Luger, R., and VanderPlas, J. T. (2020). On the xuv luminosity evolution of trappist-1. *The Astrophysical Journal*, 891(2):155.

Gallet, F., Charbonnel, C., Amard, L., Brun, S., Palacios, A., and Mathis, S. (2017). Impacts of stellar evolution and dynamics on the habitable zone: The role of rotation and magnetic activity. *Astronomy & Astrophysics*, 597:A14.

Gillon, M., Jehin, E., Lederer, S. M., Delrez, L., de Wit, J., Burdanov, A., Van Grootel, V., Burgasser, A. J., Triaud, A. H., Opitom, C., et al. (2016). Temperate earth-sized planets transiting a nearby ultracool dwarf star. *Nature*, 533(7602):221–224.

Gonzalez, G., Brownlee, D., and Ward, P. (2001). The galactic habitable zone: galactic chemical evolution. *Icarus*, 152(1):185–200.

Gordon, R. and Sharov, A. (2017). *Habitability of the Universe before Earth: Astrobiology: Exploring Life on Earth and Beyond (series)*. Academic Press.

Hanslmeier, A. (2010). *Water in the Universe*, volume 368. Springer Science & Business Media.

Hauschildt, P. H., Allard, F., Ferguson, J., Baron, E., and Alexander, D. R. (1999). The nextgen model atmosphere grid. ii. spherically symmetric model atmospheres for giant stars with effective temperatures between 3000 and 6800 k. *The Astrophysical Journal*, 525(2):871.

Heath, M. J., Doyle, L. R., Joshi, M. M., and Haberle, R. M. (1999). Habitability of planets around red dwarf stars. *Origins of Life and Evolution of the Biosphere*, 29:405–424.

Hunten, D. M., Pepin, R. O., and Walker, J. C. (1987). Mass fractionation in hydrodynamic escape. *Icarus*, 69(3):532–549.

Irion, R. (2002). Astrobiologists try to'follow the water to life'.

Joshi, M., Haberle, R., and Reynolds, R. (1997). Simulations of the atmospheres of synchronously rotating terrestrial planets orbiting m dwarfs: conditions for atmospheric collapse and the implications for habitability. *Icarus*, 129(2):450–465.

Kasting, J. F. and Catling, D. (2003). Evolution of a habitable planet. *Annual Review of Astronomy and Astrophysics*, 41(1):429–463.

Kopparapu, R., Wolf, E. T., Haqq-Misra, J., Yang, J., Kasting, J. F., Meadows, V., Terrien, R., and Mahadevan, S. (2016). The inner edge of the habitable zone for synchronously rotating planets around low-mass stars using general circulation models. *The Astrophysical Journal*, 819(1):84.

Kopparapu, R. K., Ramirez, R., Kasting, J. F., Eymet, V., Robinson, T. D., Mahadevan, S., Terrien, R. C., Domagal-Goldman, S., Meadows, V., and Deshpande, R. (2013). Habitable zones around main-sequence stars: new estimates. *The Astrophysical Journal*, 765(2):131.

Krissansen-Totton, J. and Fortney, J. J. (2022). Predictions for observable atmospheres of trappist-1 planets from a fully coupled atmosphere–interior evolution model. *The Astrophysical Journal*, 933(1):115.

Laughlin, G., Bodenheimer, P., and Adams, F. C. (1997). The end of the main sequence. *The Astrophysical Journal*, 482(1):420.

Lim, O., Benneke, B., Doyon, R., MacDonald, R. J., Piaulet, C., Artigau, É., Coulombe, L.-P., Radica, M., L'Heureux, A., Albert, L., et al. (2023). Atmospheric reconnaissance of trappist-1 b with jwst/niriss: Evidence for strong stellar contamination in the transmission spectra. *The Astrophysical Journal Letters*, 955(1):L22.

Lissauer, J. J. (2007). Planets formed in habitable zones of m dwarf stars probably are deficient in volatiles. *The Astrophysical Journal*, 660(2):L149.

Luger, R. and Barnes, R. (2015). Extreme water loss and abiotic o2 buildup on planets throughout the habitable zones of m dwarfs. *Astrobiology*, 15(2):119–143.

Luger, R., Barnes, R., Lopez, E., Fortney, J., Jackson, B., and Meadows, V. (2015). Habitable evaporated cores: transforming mini-neptunes into super-earths in the habitable zones of m dwarfs. *Astrobiology*, 15(1):57–88.

Lynden-Bell, R. M., Morris, S. C., Barrow, J. D., Finney, J. L., and Harper, C. (2010). *Water and life: the unique properties of H2O*. CRC Press.

Mann, A. W., Wood, M. L., Schmidt, S. P., Barber, M. G., Owen, J. E., Tofflemire, B. M., Newton, E. R., Mamajek, E. E., Bush, J. L., Mace, G. N., et al. (2022). Tess hunt for young and maturing exoplanets (thyme). vi. an 11 myr giant planet transiting a very-low-mass star in lower centaurus crux. *The Astronomical Journal*, 163(4):156.

Matsuo, T., Shibai, H., Ootsubo, T., and Tamura, M. (2007). Planetary formation scenarios revisited: Core-accretion versus disk instability. *The Astrophysical Journal*, 662(2):1282.

Mottl, M. J., Glazer, B. T., Kaiser, R. I., and Meech, K. J. (2007). Water and astrobiology. *Geochemistry*, 67(4):253–282.

Owen, J. E. and Alvarez, M. A. (2015). Uv driven evaporation of close-in planets: Energy-limited, recombination-limited, and photon-limited flows. *The Astrophysical Journal*, 816(1):34.

Pascal, R., Boiteau, L., Forterre, P., Gargaud, M., Lazcano, A., Lopez-Garcia, P., Moreira, D., Maurel, M.-C., Pereto, J., Prieur, D., et al. (2006). Prebiotic chemistry—biochemistry—emergence of life (4.4-2 ga). *From Suns to Life: A Chronological Approach to the History of Life on Earth*, pages 153–203.

Pollack, J. B., Hubickyj, O., Bodenheimer, P., Lissauer, J. J., Podolak, M., and Greenzweig, Y. (1996). Formation of the giant planets by concurrent accretion of solids and gas. *icarus*, 124(1):62–85.

Rampelotto, P., Gordon, R., Seckbach, J., and Sharov, A. A. (2018). Habitability of the universe before earth.

Raymond, S. N., Quinn, T., and Lunine, J. I. (2004). Making other earths: dynamical simulations of terrestrial planet formation and water delivery. *Icarus*, 168(1):1–17.

Ribas, I., Bolmont, E., Selsis, F., Reiners, A., Leconte, J., Raymond, S. N., Engle, S. G., Guinan, E. F., Morin, J., Turbet, M., et al. (2016). The habitability of proxima centauri b-i. irradiation, rotation and volatile inventory from formation to the present. *Astronomy & Astrophysics*, 596:A111.

Roettenbacher, R. M. and Kane, S. R. (2017). The stellar activity of trappist-1 and consequences for the planetary atmospheres. *The Astrophysical Journal*, 851(2):77.

Rogers, L. A. (2015). Most 1.6 earth-radius planets are not rocky. *The Astrophysical Journal*, 801(1):41.

Saar, S. H., Butler, R. P., and Marcy, G. W. (1998). Magnetic activity-related radial velocity variations in cool stars: first results from the lick extrasolar planet survey. *The Astrophysical Journal*, 498(2):L153.

Scalo, J., Kaltenegger, L., Segura, A., Fridlund, M., Ribas, I., Kulikov, Y. N., Grenfell, J. L., Rauer, H., Odert, P., Leitzinger, M., et al. (2007). M stars as targets for terrestrial exoplanet searches and biosignature detection. *Astrobiology*, 7(1):85–166.

Soliz, J. J. (2023). *Low Levels of Photosynthetically Active Radiation on Trappist-1e Implies No Complex Life*. PhD thesis, San Diego State University.

Somers, G., Cao, L., and Pinsonneault, M. H. (2020). The spots models: a grid of theoretical stellar evolution tracks and isochrones for testing the effects of starspots on structure and colors. *The Astrophysical Journal*, 891(1):29.

Squicciarini, V., Claudi, R., and La Rocca, N. (2021). Searching for the oxygen footprint of light-harvesting organisms. Technical report, Copernicus Meetings.

Triaud, A. H., Gillon, M., Selsis, F., Winn, J. N., Demory, B.-O., Artigau, E., Laughlin, G. P., Seager, S., Helling, C., Mayor, M., et al. (2013). A search for rocky planets transiting brown dwarfs. *arXiv preprint arXiv:1304.7248*.

Turbet, M., Bolmont, E., Leconte, J., Forget, F., Selsis, F., Tobie, G., Caldas, A., Naar, J., and Gillon, M. (2017). Modelling climate diversity, tidal dynamics and the fate of volatiles on trappist-1 planets. *arXiv preprint arXiv:1707.06927*.

Vida, K., Kővári, Z., Pál, A., Oláh, K., and Kriskovics, L. (2017). Frequent flaring in the trappist-1 system—unsuited for life? *The Astrophysical Journal*, 841(2):124.

Weiss, L. M. and Marcy, G. W. (2014). The mass–radius relation for 65 exoplanets smaller than 4 earth radii. *The Astrophysical Journal Letters*, 783(1):L6.

Wheatley, P. J., Louden, T., Bourrier, V., Ehrenreich, D., and Gillon, M. (2017). Strong xuv irradiation of the earth-sized exoplanets orbiting the ultracool dwarf trappist-1. *Monthly Notices of the Royal Astronomical Society: Letters*, 465(1):L74–L78.

Wolf, E. and Toon, O. (2010). Fractal organic hazes provided an ultraviolet shield for early earth. *Science*, 328(5983):1266–1268.

Wordsworth, R. and Pierrehumbert, R. (2014). Abiotic oxygen-dominated atmospheres on terrestrial habitable zone planets. *The Astrophysical Journal Letters*, 785(2):L20.

Yang, J., Cowan, N. B., and Abbot, D. S. (2013). Stabilizing cloud feedback dramatically expands the habitable zone of tidally locked planets. *The Astrophysical Journal Letters*, 771(2):L45.